# THE CENTRAL TENDENCY RELATIONSHIPS BETWEEN EARTHQUAKES, QUANTUM FLUCTUATIONS, AND THE HUMAN BRAIN

by

DAVID A. E. VARES

A thesis submitted in partial fulfillment
of the requirements for the degree of
Master of Arts (MA) in Psychology

The Faculty of Graduate Studies
Laurentian University
Sudbury, Ontario, Canada

**THESIS DEFENCE COMMITTEE/COMITÉ DE SOUTENANCE DE THÈSE**
**Laurentian Université/Université Laurentienne**
Faculty of Graduate Studies/Faculté des études supérieures

Title of Thesis
Titre de la thèse: The Central Tendency Relationships Between Earthquakes, Quantam Fluctuations, and the Human Brain

Name of Candidate
Nom du candidat: Vares, David

Degree
Diplôme: Master of Arts

Department/Program
Département/Programme: Psychology

Date of Defence
Date de la soutenance: September 12, 2014

**APPROVED/APPROUVÉ**

Thesis Examiners/Examinateurs de thèse:

Dr. Michael Persinger
(Supervisor/Directeur(trice) de thèse)

Dr. Cynthia Whissell
(Committee member/Membre du comité)

Dr. Ratvinder Grewal
(Committee member/Membre du comité)

Dr. Matti Pitkänen
(External Examiner/Examinateur externe)

Approved for the Faculty of Graduate Studies
Approuvé pour la Faculté des études supérieures
Dr. David Lesbarrères
M. David Lesbarrères
Acting Dean, Faculty of Graduate Studies
Doyen, Faculté des études supérieures

**ACCESSIBILITY CLAUSE AND PERMISSION TO USE**

## Abstract

Physical phenomena occur within a complex manifold of interactions from small scale quantum to large scale energies. These random interactions appear to conform to the central limit theorem, however prediction of these events suggest a non-local factor is typically involved. Data were compiled from a random number generator that utilizes quantum electron tunneling, a photomultiplier tube measuring background photon emissions (~$10^{-11}$ W/$m^2$), earthquakes recorded by USGS Advanced National Seismic System, and from a database of human electroencephalographic recordings. The data indicated temporal and spatial relationships, suggesting the causality of physical phenomena and the associated entropy conforms to the central limit theorem by means of variable distribution of occurrence.



## Keywords

Memory, Consciousness, Quantum Randomness, Entropy, Photons, Semiconductor, Quantum Random Number Generation, Causality, Specious Present, Low Magnitude Earthquake Frequency, Gaussian Distribution, Central Limit Theorem, Planck's Length Energy, Zero Point Fluctuation Frequencies, Quantum Geophysical Effects, Electroencephalography, Background Photon Fluctuation, Earthquake Energy

## Co-Authorship Statement

Peer-reviewed papers included in this thesis document were co-authored by Dr. M. A. Persinger, and are indicated accordingly.

## Acknowledgments

The author would like to acknowledge the guidance received from:

Supervisor, Dr. Michael Persinger

Thesis Committee, Dr. Cynthia Whissell

Thesis Committee, Dr.  Ratvinder Grewal

Technician, Professor Stan Koren

Fellow Colleagues from the Laurentian University, Neuroscience Research Group

Fellow Colleagues from the Laurentian University, Psychology Department

Confidants, Friends, Family and Laryssa

# Table of Contents

# List of Tables

# List of Figures

# Chapter 1

# 1 Introduction

## 1.1 Representations of Reality within the Human Brain

Two units comprise the fundamental universe; space and time. These identities are always changing, and comprise the elemental structure of human memory. The representation of memory can be considered as a continual transformation of electromagnetic functions for neuronal action potential representation. Different spine generation changes with environmental experience (Greenough, 1984), and serve as the structural mechanisms of mental representations. The brain efficiently recognizes patterns which represent reality. Memory is a consolidated pattern of a reality perception. Pattern recognition depends upon acquisition and recollection of complex procedural knowledge. This complex procedural knowledge is therefore, subject to the limitations of the brain. Understanding the seemingly random functional connections between extensive dendritic branching distributions, and the random interaction of representations of physical experience and phenomena is the focus of this paper.

The dendritic surface area is 20 to 100 times larger than that of the neuron soma (up to half of this dendritic surface area is comprised of spines), and with Ohm's Law, the charge to the neuron decreases as the spine-stem resistance increases (Rall & Segev, 1988). A change in the spine shape would thus modify the functional electrical resistance. Shortening or widening changes to this postsynaptic density (PSD) constitutes such electrical efficacy which may be the source of structural neuronal plasticity, appear to oscillate with modifications to synaptic function (Nikonenko et.al., 2002). Spines may form either from dendritic shafts, or from transformed 'filopodia' (Dailey & Smith, 1996). Synaptic activation resulting in long-term potentiation (LTP), typically begin within 10 – 15 minutes of dendritic filopodia growths (Maletic-Savatic et.al., 1999). After elongations and retractions of the filopodia the immergence of new PSDs becomes plausible. Production of filopodia is calcium dependent and NMDA sensitive (Maletic-

Savatic et.al., 1999), and takes approximately 10 - 15 minutes for growth into a bouton, complete with vesicles (Koch et. al., 1992).

An average spine head volume of 0.001 $\mu m^3$ is attached to the neuronal dendrite by a thin diameter <0.1μm neck (Nimchinsky et. al., 2002). Assuming 5 – 20 millisecond transmission, and applying Avogadro's number, there is approximately one $Ca^+$ ion is present in the channel at any given time. Synaptic stimulation can lead to $Ca^{2+}$ influx, and are found predominantly in the geometry of $4^{th}$ and $5^{th}$ order splitting of dendritic arborizations. Dendritic spine growth is mostly distal to the soma and found predominantly in the thinner diameters further along the dendritic orders. The notion that dendritic arborizations may be fractal in nature has yet to be identified. Yet there are some physical natures of the spine that can be addressed. Because the $Ca^{2+}$ currents evoking a single action potential decay in less than 20 msec, and diffusion time across the spine neck is approximately 100 msec, at least 5 stimulations separated by no more than 20 msec are required to maintain the Ca2+ stream (Nimchinsky et. al., 2002). The volume of the spine serves to collect the calcium ions from the spine head down the neck (Koch et. al., 1992). With a thin spine neck, more time is required for conductivity. With a thick spine neck, less time is required for conductivity. Therefore, the thickness of the spine neck can be thought of as a mechanism of tuning in the conductance of signaled information.

Disappearance of spines occurs randomly in time and space (Engert & Bonhoeffer, 1999). This may play a role in the adaptation to the random environment of which the brain exists. By being flexible beyond a static representation, the quantum nature of the environment may have potential representation via entangled or shared states with the dynamic dendritic surface. Filopodia oscillate between 50% – 60% existence and extinction over a 4 hour period. The environment to which the brain is subjected has been shown to dictate the quantity of spine formation densities per neuron. This oscillation of filopodia is detectable by the human eye, and can be therefore assumed to have rates that are below the flicker fusion threshold around 20 – 30 Hz (Alpern et. al., 1953). Another possible role of dendritic filopodia may serve to pick up signals (chemical) from the gaseous environment within 'brain space'.

A significant increased spine density in CA1 basal dendrites was evident for spatially trained rats, as compared to controls (Moser et. al., 1994) with an upwards density of 1.96 ± 0.09 spines per µm. Assuming the average surface area of a cell is 3.14 x $10^{-10}$ $m^2$, this averages out to an increase of 600 new spines per cell. There is thus the possibility that the CA1 (along with responding to direct entorhinal cortex information) melds information into the spatial representations as received from the CA3 which is encoded with reference to the current environmental context (Bilkey, 2004). Similar to the orientation cells of the visual cortex, environmental 'place cells', would be necessarily context dependent of the CA3 information. Memory is therefore highly dependent upon context.

Along with the spatial components of memory, meaning components are highly integrated. The state equivalent of context would be emotion. From the hippocampus to the cortex, current signals are coded with ripples of rhythm. Current generators are transmembrane currents creating the magnitude of the field, while the term rhythm generator refers to the mechanisms responsible for oscillatory pattern and frequency (Buzsaki, 2002). The proposal that the CA3 region functions as an intrahippocampal theta oscillator, although lesions of the medial-septum-diagonal band of Broca (MS-DBB) eliminates theta waves may be the ultimate rhythm generator (Petsche et. al., 1962). The difference between LTP memory consolidation and long-term depression (LTD), is LTP is phosphorylation, while LDP is dephosphorylation, and with simultaneous induction at different synapses which may serve to cancel one another out (Whitlock et. al., 2006). These current signals typically consist of a ripple of gamma (40+ Hz), piggybacked on the fundamental theta waves (4 – 7Hz). Taking the bulk velocity of signal transmission (4.5 m/s), divided by the circumference of the cortex (0.6 m), a resonance frequency of 7 Hz is the result. Complimentarily, taking the bulk velocity (4.5 m/s) and the rostral caudal cycle during one 20 msec duration (approximately 0.1 m), a resonance frequency of 45 Hz is the result. The fundamental frequencies seem to have been built upon the very physical structures of the human brain.

Information is modality independent, but relies on the frequency pattern. The seemingly random representations of reality are comprised of these variable frequency patterns. Memory formation is derived from protein synthesis, yet the secondary messengers that trigger the growth, take time

to affect the DNA. The repetitious patterns of stimulation, causes neurons to grow specific patterns of dendrites and axons, while new experiences carry potential variations upon the original (Ross & Redpath, 2009). During sleep, memory consolidation of the contextually dependent events takes place. While sleeping, inputs from the hippocampus recreate similar context dependent versions of the day's events in the neocortex. With repeated episodes of sleep, permanent memory representations are formed (Sejnowski & Destexhe, 2000).

Mach & Persinger (2009) showed that specifically patterned magnetic fields would produce changes in behavior, especially significant difference when applied during states of associated with synaptic plasticity (Mach & Persinger, 2009). They showed that simultaneous exposure to LTP-patterned magnetic fields while learning to inhibit, increased the accuracy of performance. Specifically, the hippocampus, amygdala, entorhinal cortex, and parietal cortex are primarily active during the first few days (Izquierdo & Medina, 1997). Memory remains in electrical format for the first 15 – 20 minutes, but changes into chemical/physical DC potentials during 3 days. Therefore, the applications of weak-intensity, specifically patterned magnetic fields applied to entire cortex, affecting behavioural performance of a learned task is confirmed. What random fields are affecting the random filopodia/PSD growth and disappearances? Brain-space must play a crucial role in representations of reality.

## 1.2 Conscious Awareness of Representations of Reality

Assuming the physical structure of the brain dictates the function of memory and perception, the continuous perceptions of reality, which combine to create the stream of consciousness, must also be reliant on the physical structure. Indeed, one may argue that the very stream of consciousness is but a mere perception of what has already happened, a simple memory of what happened, or of what was perceived by the senses a few milliseconds prior. To investigate the relationships associated with consciousness fruition, reference to the previously mentioned structure and function of the dendritic spines is essential.

Small amplitude changes in shape of spines are detectable over the course of seconds, while the diffusional exchange of the spine head and the dendrite ranges from 20ms to 200ms (Nimchinsky

et. al., 2002). Maintenance of memories even in the small millisecond ranges, include two streams responsible for 'what' and 'where'. The occipitotemporal pathway (ventral stream) maintains the identification of objects, while the occipitoparietal pathway (dorsal stream) maintains visual spatial guidance (Ungerleider, 1995). With continual sensory input from the environment, a distributed memory system underlies the conscious streams. With this understanding, the concept of memory in relation to consciousness change is merely the encoding of the individual that perspective consciousness resides (John, 1986).

The context under which the stimulus/event is observed dictates the perspective encoding. A stimulus will be considered and encoded as novel because it was either never seen before, or is observed in a new/unexpected context (Berns et. al., 1997). Different regions are activated to encode the information accordingly, and the consolidation of this information is different across gender, age, and social condition. A study of face recognition showed four regions of the brain with significant activation during encoding in the right prefrontal cortex, the right parietal cortex, and the bilateral ventral occipital cortices (Grady et. al., 1995). Important to note, right prefrontal memory is a reorganization of context dependency, especially during recognition of stimuli. The left prefrontal cortex underlies a self-referenced perceptual experience which includes both environmental and internal events within the context of the stimulus event (Wheeler et. al., 1997). It is such that the merging of memory and the development of self-awareness to create consciousness involves remembering encoded information rooted in auto-noetic awareness. Re-experiencing episodic events in a study of mental time travel demonstrated common and distinct electrophysiological correlates (Lavallee & Persinger, 2010). The process of remembering serves to provide the individual with a temporal structure for physical events upon which the different streams of conscious awareness and the sense of self are dependent.

The complexity of the electric activity of the brain requires a specialized measure. Wackermann treated the brain with such an understanding and developed a measure for space (global field strength - μV) which is a quantified measure of the overall potential variance across electrodes (Koenig et. al., 2002), time (global frequency of field changes – Hz), and complexity (dimensionless spatial complexity), where by the combinations of these measures provided an in depth look at sleep and waking states (Wackermann, 1999). This global 'holistic' measure of

brain activity provided the conceptual relationship and proportions of the brain's complexity. These microstates have been utilized to illustrate a high resolution of stable, repeating, basic building blocks of conscious processing (Koenig et. al., 2002). The relationships between 'what was just thought' and the external microstate measures have noticeable differences, for example when comparing the 2 seconds before a stimulus prompt and the experience (Lehmann et. al., 1998). The millisecond electric potential changes as measured from the scalp reflect the interactions between the environment and internal information.

The analysis of global electric potentials aids with the interpretation of conscious stream. It is a universal concept, such that the pattern of one electrode is an interaction with the global field. Magnetoencephalographic recordings have demonstrated a global 40 Hz response during sensory input (Llinas et.al., 1991). Thus consciousness can be interpreted as being both integrated and differentiated simultaneously (Tononi & Edelman, 1998). This aggregate of individual neuronal action potentials summed under the whole cerebrum has the intrinsic requirements for the criteria of a hologram (Persinger & Lavallee, 2012). The harmonic electromagnetic fields throughout the cerebral cortex encode the information stored, with coherent alignment, functioning in a uniform state (Di Biase, 2009).

Schumann resonances were originally investigated by examining neocortical surface area with the fundamental frequency estimated within the alpha brain wave range of 7 – 18 Hz (Nunez, 1995). The fundamental Schumann resonance (7.8 Hz) is recognized within the Earth's atmosphere, lithosphere, and ionosphere (Persinger, 1999). If one assumes a coherent alignment with the Earth's informational electromagnetic field and assuming the average energy density of brain space is congruent with the energy density of the entire universe, then the holographic conditions of consciousness cannot be dismissed (Persinger, 2011). With the holographic assumption bolstered by congruent harmonic resonances with the environment and universe dimensions, the concept of consciousness as an individual process diminishes. What is left is the concept that consciousness is a universal constant, and the individual is a conduit of the process. Or rather, the perception of consciousness is due to the processing of universal events within the structure of the individual brain space.

## 1.3 The Property of Randomness within Reality

The universe can be considered a vibrating manifold of quantum superposition. Assuming the universe originated from a 'Big Bang', and then consequentially, every particle that exists was once contained within a singularity. Originating from one singularity every particle in existence is necessarily entangled with every other particle in existence. Quantum entanglement (under this concept), is a universal constant. The interactions of the pre-existing entangled states, especially photons which do not experience time, would also permit a universally holographic state, to which consciousness would reside. The observation, creation and manipulation of a photon in the present, would affect the entangled from the past. Acquisition of information from a distance is the precise process of consciousness (Persinger & Lavallee, 2010). Observation of the environment, informational stimuli, and conscious representation within the individual, all manifested from the 'action at a distance', would be permitted via the pre-existing entanglement of the universe.

The information (entropy) of our environment is consolidated within the brain-space manifold. Advancements in quantum mechanics have begun to produce devices that harness the 'spooky action' of our perceived reality. In metals, there is at least one band in which the available quantum states are only partially filled. A forbidden band (energy gap) separates an uppermost filled band from the lowest most empty band. If the energy gap is small enough, thermally excited electrons can transfer from top states (filled valence band) to unoccupied bottom states (conduction band). The basic building block of Semiconductor devices is the interaction of an 'n type' solid with a 'p type' solid. The 'n type' solid is classified as having 5 or more valence electrons usually from added impurity atoms (also known as Donors). The 'p type' solid is classified as having 3 or less valence electrons where the resulting bonds between atoms are short, and vacancies exist (also known as Acceptors).

The Esaki Diode (Esaki, 1958) harnesses the internal field emission of very narrow p-n junctions with required specific impurity content of solids and a specific width of junction. The impurity solids are typically silicon and germanium. Before joining two such materials, there is no net charge in either p-n region. When the two are joined, holes and electrons in the vicinity of the junction diffuse across and the neutral charge is lost and is thus sufficient enough to prevent any

further diffusion across the junction. The width of the junction between two opposite impurity content p-n solids, is known as a barrier/boundary or depletion region. There is an electric potential difference in highly doped p-n junctions that can be calculated by:

$$V_d = \left(\frac{kT}{q}\right) \ln\left(N_n \frac{P_p}{{N_i}^2}\right)$$

where: $P_p$ = density of free hole in 'p type' solid, $N_n$ = density of free electron in 'n type' solid, and $N_i$ = density of intrinsic hole-electron pairs. Although the potential difference across the p-n regions exists at the barrier, externally no voltage can be measured across the junction. However, one can make quantitative observations when the p-n junction is 'Forward Biased' or 'Reverse Biased'. This effect results in a current-voltage relation of a p-n junction. Tunnel diodes have resulting quantum mechanical tunneling in addition to the p-n junction phenomenon and is evident under 'Reverse Biased' and 'Small Forward-Biased' conditions.

Quantum mechanical tunneling is the ability of an electron to penetrate the potential barrier and appear on the other side of the gap junction without any loss of energy. Essentially, if the externally applied 'Biased' electric field is sufficiently large, there exists the quantum wave function state possibility of a transition of electrons from the valence band, into quantum states of like energy in the conduction band. The actual number of electron transitions per second is calculated by multiplying the probability of tunneling by the number of electrons striking the barrier per second. The magnitude of the barrier field is inversely proportional to the barrier width. When the field reaches a certain magnitude, a sudden increase of transitions occur (valence band to conduction band).

"Random walks" are fundamental to Markov processes. The outcome of a random coin toss has two possibilities, "heads" or "tails". Because the outcomes from any previous coin tosses are independent of the next, the probability of obtaining heads vs. tails will always remain 50/50 regardless of any information obtained from past toss outcomes. Thus a memory less, stochastic process is called a Markov process, and by the central limit theorem any repeated stochastic

processes will lead to a Gaussian distribution. It is important to note the term 'memory less' process.

When light strikes a semiconductor it supplies energy to knock electrons free of their atomic orbits, creating holes and electrons. This light sensitive behavior occurs in the depletion zone of a reverse biased diode. The phototransistor behaves the same way when light impinges upon its reverse biased collector-base junction depletion layer. Of course the transistor amplifies this current so that a much larger current flows in the collector-emitter circuit than in diode. Lenses are used to enhance the light sensitivity.

Living cells emitted photonic radiation with wavelengths within the 190 nm to 5000 nm range at between $10^5$ and $10^7$ photons/$m^2$ second. With any superposition of states, a new state shares properties of the composing states regardless of space or time. Entanglement or excess correlation allows quantum communications: (i.e., change in polarity of one previously proximal photon results in reverse polarity of the other at any distance).

Absorption of photons leads to excess electrons in the n-side and excess holes in the p-side, generating a voltage drop across the p-n junction. Absorbed photons outside the depletion region are not be separated by the electrostatic field potentials and once the carriers lifetime has elapsed, they will recombine spontaneously, emitting photons having a total energy equal to the energy gap. New photo diodes have 'p' doped region measuring approximately 13 μm by 2500 μm (2.5 mm) that serves as the cathode.

The "random" nature of our immediate and local environment is not only microscopic. At the center of any solar system is a quantum event generator. A proton-proton cycle produces energy within the star's core in the form of neutrinos and radiation; $[4\,^1H + 2\beta^- \rightarrow {}^4He + 2\,\nu + 6\,\gamma]$. Due to weak interactions with matter, neutrinos escape without much trouble, but as in the case of our Sun's radius, gamma radiation interacts with nearly 700,000 km of matter. Due to the conservation of energy and momentum, a photon bumping into an electron changes its path and time is required to reach the surface. Computer simulations of the photon's quantum random walk from the center of our Sun's core traveling to the surface, is estimated to take anywhere

from (4.9 ± 1.4) x $10^4$ years for a solar constant density, and (2.9 ± 0.57) x $10^6$ years for a linearly decreasing density. Immerging from the Sun's photosphere, an Earth bound photon takes an approximate 8 minutes to reach us. Reflection/radiation continually occurs, but the majority of photons destined for Earth undergo atmospheric refraction. The Earth absorbs 1.1 x $10^{17}$ J/s of power from the sun. The estimated temperature of the Earth during the day is approximately 300 K, while at night is around 285 K.

In general the barriers that occur in physical phenomena (both semiconductors and synaptic gap junctions) are not square and so we can obtain an approximate expression for the transmission coefficient through an irregular barrier. The only solution is to treat a smooth, curved barrier (the potential is a slowly function of *x*) as a series of square barriers. With the integration over the region in which the square root is real, so is it for the tunneling conditions.

Radially oriented (gyral) electric dipoles project to the scalp surface, but their magnetic fields remain tangentially oriented with respect to the scalp surface and appear at some distance from the dipole generating them. Tangentially oriented (sulcal) electric dipoles do not project to the scalp surface directly overlying them, but their magnetic fields do. Electrical dipoles are attenuated and diffused by the tissues through which they must pass before appearing at the scalp surface; magnetic fields do not exhibit this attenuation and diffusion, but their strength diminishes at $1/r^2$, where r = radius from the dipole source.

The concept of a local hidden variable is commonly used in the EPR paradox and Bell's inequality. In quantum mechanics, this is the assumed notion that distant events have no instantaneous effect on local (and isolated) events, following the strict obligation that nothing can travel faster than the limit of velocity for EM photon propagation. In quantum entanglement theory, the hidden variable explains the Schrödinger wave function state vector collapsing from a probability (before measurement) into a certainty (after measurement). Although useful for quantum calculations, the hidden variable still plagues scientific understanding of the seemingly random nature of reality.

## 1.4 Quantum Interactions within the Manifold of Reality

A component of the phenomenon under investigation involves quantum tunneling. Despite the relatively reliable sampling rates, the quantum world is "spooky". The velocity of an incident tunneling electron wave packet becomes infinite inside a zero-time space barrier. With wave number *k* imaginary, the duration of time for the incident electron wave packet to tunneling across the potential barrier becomes zero. This phase change is a special solution of the Schrodinger wave function:

$$\Psi_I(x,t) = e^{\frac{-iEt}{\hbar}}\left[A_I e^{\frac{ipx}{\hbar}} + B_I e^{\frac{-ipx}{\hbar}}\right]$$

where; particle momentum $p = (2mE)^{-1/2}$ and $A_I$ and $B_I$ are Eigenfunctions of the momentum operators for the incident and reflected propagations of the particle in each region. During tunneling in the barrier region the corresponding wave function solution undergoes absorption. Although the energy of the instantaneously tunneled electron remains consistent, the probability amplitude is no longer the simple addition of oscillating functions but instead contains combinations of exponential ones. The phase change solutions to the special Schrodinger equations violate Einstein causality for signal transmissions. For: ($W^2 = c^2p^2$) where W = (energy), and p = (momentum), the instantaneous tunneling electron is faster than the speed of light. Quantum tunneling is therefore known as the finite probability, as determined by the ratio of coefficients of the special Schrodinger equation, of finding particles at the inflection points between.

The Psyleron REG device involves two environmentally shielded, NPN epitaxial 0.048 mg silicon transistors. Under a reversed biased current, heavily doped electrons jump across a classical barrier without loss of energy. The Heisenberg uncertainty principle grants random tunneling, translating into a varying voltage level that is processed, amplified and converted to a digital stream. The two streams from both chips are compared with a Boolean XOR procedure to eliminate environmental influence, whereby: [(11, 10, 01, 00) = (0,1,1,0)] respectively. In short, the Psyleron REG is a professional, non-classical coin flipper. These probabilities are likewise derived from the cumulative deviations that arise from the total 1s out of 200 distribution.

Modern Psyleron REG devices employ two random sources which are compared against one another using XOR (exclusive OR logic) operation that is designed to reduce the impact of physical artifacts. Further, the digital output is undergoes a bitwise Boolean XOR operation to ensure statistical randomness and creates statistical balanced REG output, even if there are physical biases in the noise source. Output data are presented and recorded in 'trials' and are the sum of 'N' samples (i.e. 200 bits), usually generated at approximately 1 bit per second.

The entire circuit is shielded by an outer aluminum enclosure, as well as with an inner perm alloy mu-metal which isolates the sensitive analog portions. This inner shield attenuates both electrical and magnetic effects from inside and outside the REG-1 device. The result of the XOR processing and the shielding precautions from multiple analog noise sources, enable Psyleron to claim that the REG-1 device is not sensitive to environmental or known physical factors. Psyleron conducts calibration tests the REG-1 device before being shipped, conforming to statistical chance expectations for mean, standard deviation, skew, and kurtosis for an accumulated count distributions (equivalently, 1 billion bits). Other tests include autocorrelation, arcsine, run length, and mean and SD tests on 100 and 1000 trial blocks. All tests evaluated against the null hypothesis that data conform to theoretical distributions for perfectly balanced processes. Due to the extensive shielding and calibration testing of the Psyleron REG-1 device, classical physical interactions can be ruled out as the source of deviation from statistical randomness.

The Psyleron REG harnesses the p-n junctions (under a reversed-biased current) and quantum mechanical tunneling to produces a varying current for RNG. Clearly the PMT measures direct hit photons, but measuring vacuum fluctuations which include Casmir and van der Waals forces should be considered with inherent pair-particle creation due to quantum vacuum fluctuations.

This superposition of electrons, quantum tunneling, and probability of wave function collapse via entanglement all involve a chance statistic. The REG-1 Psyleron device encapsulates quantum tunneling to generated random events, via electron superposition probabilities between a valence band and conduction band harnessing. The spontaneous activity of excitatory–inhibitory neuron

pairs is positively correlated, while sensory stimuli actively decorrelate joint responses. Computational modeling shows how threshold nonlinearities and local inhibition form the basis of general decorrelating mechanisms. (Ficek, 2010).

Electron behavior is governed by the Schrödinger Wave equation. The solution of the equation represents a quantum state which only one electron can occupy. This is determined by a discrete value of electron energy and behavior of that quantum state. For each value of energy of a given electron (E), the wave equation yields one or more 3D wave function solutions ($\psi$). $|\psi|^2$ = the probability of an electron being at a particular point at a given time that the wave equation ($\psi$) is being solved. When close atoms in a solid are considered, the potential energy of the electron is a complicated periodic function representing the sum of all the electric potentials contributed by every atom in the solid. The close atoms cause wave functions to overlap where each energy level splits into a number of overlapping wave functions or potential probabilities of an electron being at a particular point. The properties of a solid are determined by the extent to which available quantum states in each band are occupied.

"The phenomenon termed as sudden birth of entanglement, as it is opposite to the sudden death of entanglement, arises dynamically during the spontaneous evolution of an initially separate qubits. The sudden birth of entanglement is now intensively studied as it would provide a resource for a controlled creation of entanglement on demand in the presence of a dissipative environment." (Ficek, 2010). "The static Casimir effect describes an attractive force between two conducting plates, due to quantum fluctuations of the electromagnetic (EM) field in the intervening space. Modified fluctuations of the EM field can also account for the "van der Waals" interaction between conducting spheres, and have analogs in the fluctuation-induced interactions between inclusions on a membrane." (Kardar, 1999). The quantum mechanical tunneling is the ability of an electron to penetrate the potential barrier and appear on the other side of the junction without any loss of energy. There exists the quantum wave function state possibility of a transition of electrons from the valence band, into quantum states of like energy in the conduction band.

Applying the quantum tunneling concept to the physical brain, the gap junction of 2 nm between two communicating neurons, the potential to represent the quantum nature of reality exists. It has been argued that the physical brain is too warm and too wet an environment to support quantum superposition of particles and the non-causal nature of quantum mechanics. Yet the components of the brain are not comprised of just one time or energy scale but vary with level of spatial-temporal discourse. The whole brain is typically a hot and wet environment of 300ºK. Clearly quantum coherence must compete with these thermal fluctuations, and would collapse any superposition wave. Utilizing the equation:

$$E = \frac{1}{2} k_b T$$

where; $k_b$= Boltzmann's constant (1.38 x $10^{-23}$ $m^2$ $kg/s^2$) and Heisenberg's uncertainty relation ($\Delta p \ \Delta q \geq 2\pi$), Beck illustrated the point at which the quantal energy is well above the physiological thermal regime (Beck, 2008). Quantum processes at room temperature require signal times smaller than the picosecond. These correspond to electric transfer, or more importantly, changes in molecular bonds such as the breaking of hydrogen bridges. The values would be some interval between a femtosecond and the $10^{-16}$ s required for one orbit of an electron. Speculation remains that only the employment of ultra-short time spectroscopy can reveal the underlying quantal processes (Vos et. al., 1993).

Persinger and Koren calculated the information from hydrogen sources would occur in increments of a nanosecond (Persinger & Koren, 2007), noting also that information from even smaller temporal durations could enter the cerebral process (Tsang et. al., 2004). At smaller and smaller levels of space and increments of time, the concept of a singularity becomes relevant. Burke & Persinger postulated the mass of the DNA in the hippocampus as the gateway to memory and consciousness is merely the boundary condition between a singularity and brain space (Burke & Persinger, 2013). Again, the idea that consciousness is a universal concept with perspective of observation being relative to the structured function of the individual as a conduit is apparent. The quantum interaction is the universal representation of energy in motion.

# Chapter 2

## 2 Predicting Random Events from Background Photon Density Two Days Previously: Implications for Virtual-to-Matter Determinism and Changing the Future

**David A. E. Vares[1] and Michael A. Persinger[1]**

*1 Bioquantum Laboratory, Laurentian University, Sudbury, Ontario, Canada, P3E 2C6*

Tel: 01-705-675-4824; Fax: 01-705-671-3844

E-mail: dx_vares@laurentian.ca and mpersinger@laurentian.ca

*Journal of Nonlocality Vol II, Nr 2, December 2013 ISSN: 2167-6283*

Submitted: September 23, 2013

Accepted for Open Peer Review: December 19, 2013

**Abstract.** We tested the hypothesis that discrete energies from entropic-like processes immersed within background photon densities of ~$10^{-11}$ W·m$^{-2}$ were coupled to the occurrence of changes in random events that lead to specific consequences about two days later. This latency was obtained from the ratio of the summed equivalent energies associated with a Bohr electron divided by the value for the fluctuation of background photon density within the likely area of the gap junctions mediating the electron tunneling. Hourly values for 30 days for background photon densities and deviations on random number generators involved lags between 0 and 72 hours. Multiple regression equations indicated that deviations from random number variations were only correlated with photon densities approximately 48 hrs (2 days) previously. Convergent quantitative values were consistent with source energies from virtual particles at the level of entropic thresholds. The delay of approximately two days between the emergent energies that influence an event and the manifestation of the event in physical time or the specious present suggest that technology could be developed to predict or modify actual events in real time. Implications for causality and determinism are considered.

**Key Words:** Entropy photons semiconductor quantum random number generation causality specious present

## 2.1 Introduction

First approximations of magnitude relate the increments of space (Δs) and the increments of time (Δt) to perceptual processes (Persinger, 1999). For example, to discern phenomena dependent upon processes at the level of the atom ($10^{-12}$ m) Δts in the order of $10^{-12}$ s are required. To discern phenomena at the level of the proton or electron ($10^{-15}$ m) shorter intervals in the femtosecond ($10^{-15}$ s) are more optimal. At larger scales, in the order of megameters, that are encountered by geophysicists investigating seismicity, the Δts required to identify the most reliable and predictable patterns are in the order of $10^{6}$ s. If the optimal Δt is not employed, the phenomenon may not be detected because of excessive fragmentation, such that intercorrelations approach zero (when Δts are too narrow) or multiple phenomena are summated into aggregates as if they were singular events (when Δts are too wide).

From subatomic particles to celestial aggregates, the functional Δt is neither discrete nor fixed across levels of scientific discourse. Although artifacts of measurement or conceptual limitations of human perceptions cannot be totally eliminated, the shape of the distribution of the optimal Δt appears to be Gaussian-like. This perspective is consistent with the central limit theorem that states that if an infinite number of the means of samples of random numbers were plotted, they would display a normal distribution. Consequently the processes that contribute to the present (the vertical line in Figure 2.1) can display a wider increment than the Δt by which events are measured serially or sequentially. In this instance specious present is defined as the short time span in which duration and change are experienced or measured directly. It implies there are antecedent conditions that may display Bayesian characteristics with respect to an event when a field or flow metaphor is employed.

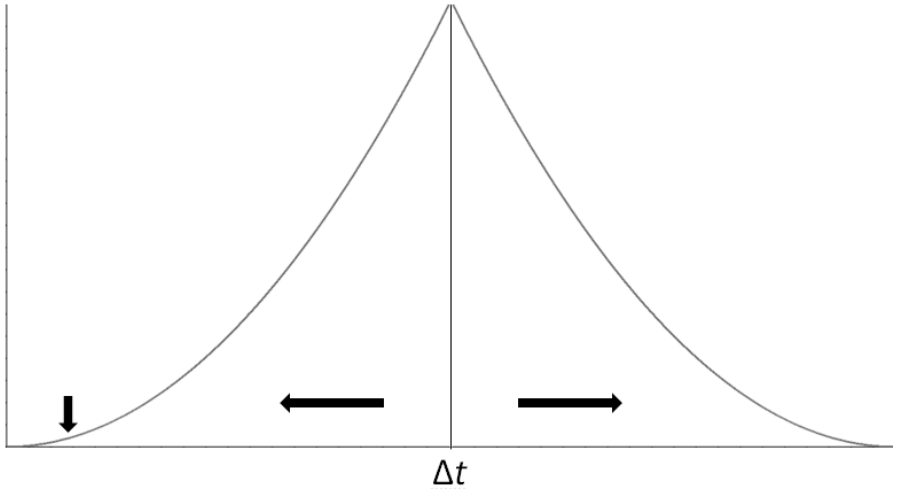


**Figure 2.1 - Representation of the specious present (vertical line) and the theoretical distribution of energies from processes that contribute to the physical event at Δt. The arrow indicates the hypothetical occurrence of energy represented as photons that emerge from "virtual" particles within background entropy. In this instance the vertical axis refers to the qualitative probability of the event occurring with a maximum at Δt.**

One of the implications of this approach is that a process coupled to entropy that occurs during the initial elevations of a probability (the arrow in Figure 2.1) above the random background that precedes an actual event: 1) is entangled with the consequent manifestation of the actual event, and, 2) determines actual events that occur as changes in the organization of matter in the specious present. The result is the occurrence of the event within the "now" temporal frame. The approach is also consistent with the concept of "the specious present" which implies that what constitutes the causal moment is actually wider and composed of subtle energetic sequences that systematically precede the physical event. The analogy might be the elevation of local electrical gradients seconds to minutes before the actual manifestation of the initiation of a leader for a lightning discharge (Persinger, 2012).

For several years we have been measuring background photon emissions (~$10^{-11}$ W/$m^2$) in a very dark basement laboratory (Dotta et al., 2011). The spectral profiles of these emissions are concurrent with the free oscillations of the earth-atmospheric interface (Persinger, 2012a) that range between 3 and 5 mHz. Marked elevations by a factor of 10 or more in the intensity of this photon density have been measured more than a week before very large *M >8.0* earthquakes that occurred later at distances of several thousands of km (Persinger et al., 2012).

We have assumed that any observable event, from the collapse of a building to the failure of a biological system, begins with a quantum of energy equivalent to a discrete value such as the shift in an electron shell or the differential between the spin and orbital magnetic moment of an electron ($\sim 10^{-26}$ A $m^2$). Because this quantity is almost identical to the magnetic moment of a proton, this concept may be relevant to processes that determine causality and the arrow of temporal sequences that might emerge from entropic sources. We designed an experiment that could potentially test the hypothesis that deviations from random variations are preceded by perturbations in the background photon emissions.

## 2.2 The Model

Random Number Generators (RNGs) are based upon the concept of electron tunneling between the $\Delta s$ separating two areas in the order of approximately 1 $\mu m^2$. The standard RNG collects 200 samples of 0/1 events per second. When these devices are allowed to run continually in non-disturbed settings, there is the occasional deviation from chance. Random samples of 84,408 RNG events were collected and the computed total number of events that were greater than ± 20 away from the mean of 100 was 478. Assuming this relation over an hour of 3600 events results in an average of approximately 20.38 times per hour occurrence. Therefore the mean for this occasional deviation change occurring per hour, which is qualitatively distinctive, is about 20 events. Quantitatively, assuming the sample mean of 100, and a standard deviation of 7, the value of occasional deviation corresponded to single scores with a z-score exceeding the absolute value of 2.86.

If what will happen, viewed as the actual event, is preceded by patterns of energy that can be measured as perturbations in photon density, then the temporal extent of this anticipation should be calculable. Based upon the asymptote of accurate predictions for complex systems such as the local manifestations of air masses (weather prediction) and the dominant numbers of "temporal" distortions reported for centuries under questionable rubrics and explanations, (Dotta & Persinger, 2009) the width of the specious present should be in the order of between 2 and 3 days. A similar duration should occur between the energy emerging from entropic processes as a

quantified energy and the photonic exchanges that produces the events. The total energy of the electron moving at the fine-structure velocity around a Bohr radius is 4.37 x $10^{-18}$ J. We assumed that one significant deviation ($z >\pm 2.86$) within the RNG was approaching or equal to this quantum. Assuming a total of 20 such deviations the total energy would be 8.74 x $10^{-17}$ J. For the antecedent photon density our photomultiplier tubes (PMTs) displayed peak-to-peak background variations of 4 to 5 x $10^{-10}$ W/$m^2$. With the cross-sectional area of the electron tunneling across the boundary in the RNG of $10^{-12}$ $m^2$ this means that there would be 4 to 5 x $10^{-22}$ J/s. The ratio of the total energy associated with the deviations from chance divided by the former value is ~1.6 x $10^5$ s or ~2 to 3 days. If this formulation is veridical, then deviations in photon density approximately two to three days previous to deviations from random variation should be most correlated. We would expect the effect sizes, the amount of shared variance, to be small and for the statistically significant variations in photon densities to *precede* rather than succeed the variation in RNG values.

## 2.3 Relevance of Electron Tunneling in RNGs

The concept of a local hidden variable is commonly used in the EPR paradox and Bell's inequality (Bell, 1964). In quantum entanglement theory, the hidden variable explains the Schrödinger wave function state vector collapsing from a probability (before measurement) into a certainty (after measurement). According to Korotaev et al. (2005) nonlocal dependence of dissipative processes can reflect entropy productions within detectors and the environment which may also serve as a basis for quantum non-locality. Considering the recent arguments that the rest mass of photons is not zero (Tu et al, 2005), there are emergent properties that could facilitate the extraction of information from the entropic domain as well as zero point fluctuation potentials into the traditional physical realm of matter of its respective $\Delta t$. In other words, before an actual event occurs in physical space-time there would be energetic antecedents one or two days previously that are entangled with and determinants of the occurrence of the event.

RNGs from Psyleron, a company that has focused on the precise development of these devices, involve quantum tunneling of electrons. Following the Heisenberg Uncertainty Principle, the probability of an electron randomly occurring on the opposite side of the gap junction barrier,

translates into a varying voltage level. The varying voltage (white noise) generated by quantum tunneling electrons is sampled from two reverse-biased transistors. The unpredictably 'high' and 'low' voltages are due to more or less electrons tunneling across the barrier (gap junction), with a spectrum +/- 1dB, from 50Hz to 20kHz. A 1 kHz cut-off attenuates frequencies, signal amplification and clipping to produce a rectangular wave with random temporal spacing. Gated sampling yields a regularly spaced sequence of random bits.

To eliminate environmental biases, the two streams from both chips undergo Boolean Exclusive-OR logic gate operation procedures, applied in alternating 1/0 patterns. Further, the entire circuit is shielded by an outer aluminum enclosure, and with an inner perm alloy mu-metal which isolates both electrical and magnetic effects from inside and outside the REG device. Esaki (1976) noted that the current in the reverse diode might only be carried by internal field emission. The barrier breakdown occurs at less than the threshold voltage for electron-hole pair production, and so an avalanche should be excluded. In short, the Psyleron REG is a professional, non-classical coin flipper with data accessed by computer via USB port. Due to the extensive shielding and calibration testing of the Psyleron REG-1 device (1 billion bits), classical physical interactions can be ruled out as the source of deviation from statistical randomness.

The velocity of an incident tunneling electron wave packet approaches infinity inside a zero-time space barrier. With wave number *k* as imaginary, the duration of time for the incident electron wave packet to tunnel across a potential barrier approaches zero. This tunneling phase change is a special solution of the Schrodinger wave function. During tunneling in the barrier region (II), the corresponding wave function solution undergoes absorption. Although the energy of the instantaneously tunneled electron remains consistent, the probability amplitude is no longer the simple addition of oscillating functions, but combinations of exponential ones (Martin & Landauer, 1992).

The phase change solutions to the special Schrodinger equations violate Einstein causality for signal transmissions through a vacuum. For: $W^2 = c^2p^2$ where; W = (energy), and p = (momentum), the instantaneous tunneling electron is faster than the speed of light (Stahlhofen & Nimtz, 2006). There exists the quantum wave function state possibility of a transition of

electrons from the valence band, into quantum states of like energy in the conduction band. Quantum tunneling is therefore known as the finite probability, as determined by the ratio of coefficients of the special Schrodinger equation, of finding particles at the inflection points between regions (I) & (II), and regions (II) & (III) (Landauer, 1989).

Photomultiplier tubes also employ the p-n junctions and the photoelectric effect of incident photon current measurement, just as the RNG harnesses quantum mechanical tunneling to produce a varying current. Absorption of photons in the PMT leads to excess electrons in the n-side and excess holes in the p-side, generating a voltage drop across the p-n barrier junction. Lenses are used to enhance the light sensitivity, such that the PMT can be inferred to measure direct-hit photons.

However influence from vacuum fluctuations which include Casimir (Bordag et al, 2001) and Van der Waals force can be considered during inherent pair-particle creation due to quantum vacuum fluctuations. An upper limit on vacuum energy density in quantum field theory is usually represented by $< 10^{-26}$ kg/m$^3$ as the residual energy of oscillators at absolute zero (Landauer, 1989). These oscillators should have wavelengths of the order of the Compton wavelength of the proton or $h/mpc$ or ~1.3 x $10^{-15}$ m. This interconnection between vacuum energy phenomena, the yet-to-be-described predictable equations for "random" processes, photon-mediated energies, loss and gain of information from entropy, and the manifestation of particles within the physical world, are intrinsic components of the model.

## 2.4 Methods and Procedures

To test the hypothesis an inclusive database from our minute-to-minute PMTs was extracted for a one month interval (19 January - 19 February, 2013). For ease of analysis the mean photon density, RNG Zscore, and global geomagnetic aa (average antipodal) index values over this interval (743, hourly increments) were computed. The aa values (nT) were included to ensure that this important third factor, which has been correlated weakly with photon emission densities in our laboratory, was not a confounding variable. Because the aa values are 3-hr increments (8 per 24 hr period) and we employed $\Delta$ts of 1 hr, there was repetition within the successive 3 hr

periods for this variable. However we assumed that if the geomagnetic interactions were conspicuous they would still be evident.

The consideration of geomagnetic activity is also relevant to its potential coupling to subtle gravitational fluctuations. Vladimirskii (1995) measured enhancements in the order of $10^{-3}$ within G (the gravitational constant) during lower geomagnetic activity. Minakov et al. (1992) have described the conversion of a plane gravitational wave into electromagnetic radiation within a terrestrial context and recently Rowlands (1992) reiterated that gravity displays a magnetic inertial component. Korotaev et al. (2005) also showed that there is a non-local dependence of dissipative processes that is reflective in geomagnetic activity. The potential interaction is important because calculations have suggested that there may be a quantitative equivalence between gravity and light (Persinger, 2012). Several empirical studies have indicated an inverse correlation between global geomagnetic activity and local photon flux densities. In general we have found that for every 1 nT increase in global geomagnetic activity (aa values) there has been an associated decrease of $0.9 \times 10^{-12}$ $W/m^2$ in photon flux density. However the standard errors of the estimates are too large to allow predictive precision.

The RNG device was purchased from Psyleron Inc. (hardware ID: RGZD750) and is designed to generate random numbers based on quantum principles. As described by Psyleron's technicians, two environmentally shielded, Fairchild NPN Epitaxial 0.048 mg Silicon Transistors (BCX70K), under a reversed biased current employed heavily doped electrons to quantum tunnel across a classical channel barrier. The authors assumed the proprietary distance of the gap junction barrier is of the order of 1 μm. The RNG was located about 20 m distance from the Photomultiplier Tube (PMT) system which was composed of a Model 15 Photometer from SRI Instruments (Pacific Photometric Instruments) and the PMT housing (BCA IP21) for a RCA electron tube that had been employed in several other experiments involving photonic phenomena. The distance is well within the domain of non-local effects described by Korotaev et al. (2005).

The sensor of the PMT was housed in a thick wooden black box covered with several layers of black terry cloth (towels). It was connected to the photometer (scale 1 to 100) whose voltages has been recorded by a IBM laptop computer once per minute, 24 hours per day for the last three

years. Two different methods of calibration have indicated that a 1 unit change is equivalent to ~5 x $10^{-11}$ W/$m^2$. At the typical setting the range from "background" variations over several days, assuming there are no very intense imminent large (Magnitude > 8.0) global earthquakes, is between 45 and 55 units. Within a single hour the range variation around the central tendency was between 5 and 6 units. The room, in which the PMT was maintained, was sealed from light.

A total of 72 lags (3 days) were computed by software (SPSS 16 PC) for each variable. Because there were 743 cases (serial numbers of adjacent hours), this not considered a significant challenge of the degrees of freedom. Pearson (parametric) and Spearman rho (non-parametric) correlations were obtained for these lags and the other zero-lagged variables. To minimize redundancy, multiple regression analyses were completed with the numbers of deviations for the RNG as the dependent variable and the lags for the PMT as independent variables (and vice versa). Covariance for geomagnetic activity was also completed between the RNG and photon flux density data. Because of the larger number of variables involved we set the p value for entry and statistical significance into the equations at $p < 0.01$.

## 2.5 Results

The grand means, standard deviations, maximum occurring and minimum occurring values for the 743 hourly cases are listed in Table 2.1.

| **Hourly** | **Mean** | **SD** | **Max** | **Min** |
|---|---|---|---|---|
| **Value per second (of 200 1s or 0s)** | 99.9945 | .1228 | 100.3397 | 99.6606 |
| **SD Value 1s per second** | 7.0693 | .0806 | 7.3152 | 6.8155 |
| **Stouffer's Cumulative Zscore** | -.0467 | 1.0411 | 2.8826 | -2.8803 |
| **Max value per second** | 125.3100 | 2.1310 | 135 | 121 |
| **Min value per second** | 74.7000 | 2.2580 | 80 | 65 |
| **PMT photon units** | 51.8549 | 2.3707 | 59.0100 | 45.5300 |

**Table 2.1 – Means and standard deviations of hourly Random Number Generator and Units from the Photomultiplier Tube. PMT unit is 5 x $10^{-11}$ W/$m^2$.**

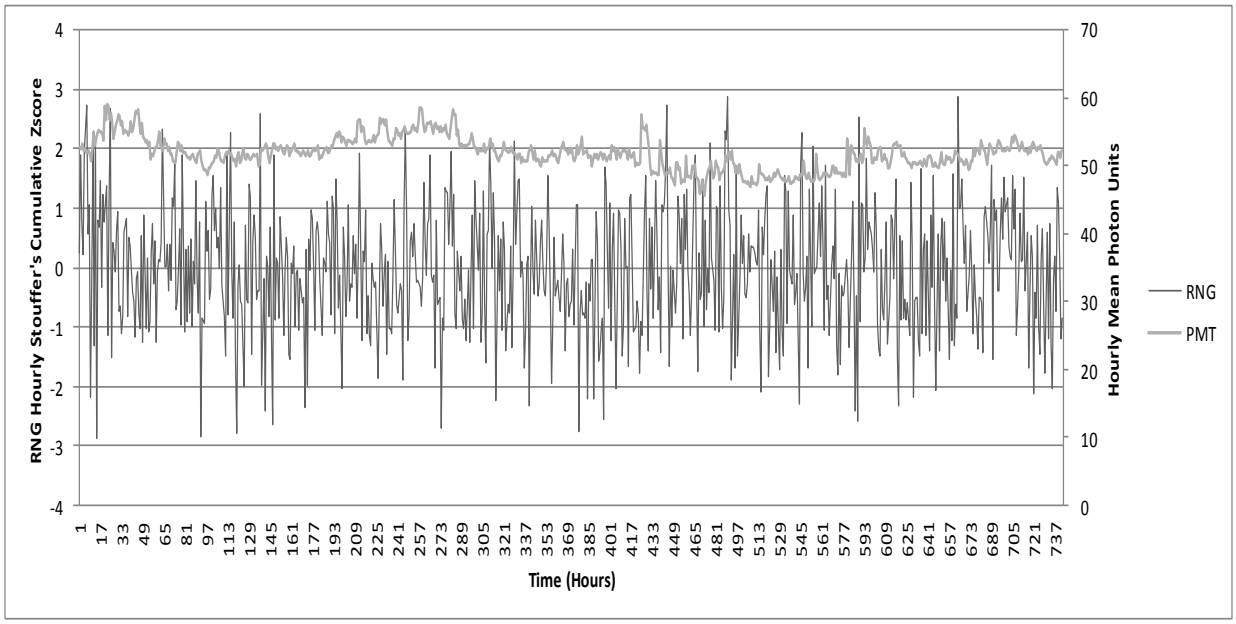


**Figure 2.2 – Display of the hourly values from January 19th, 2013 – February 19th, 2013 for the Stouffer's Cumulative Zscore of the Random Number Generating REG Psyleron device and the Model 15 Photometer from SRI Instruments (Pacific Photometric Instruments).**

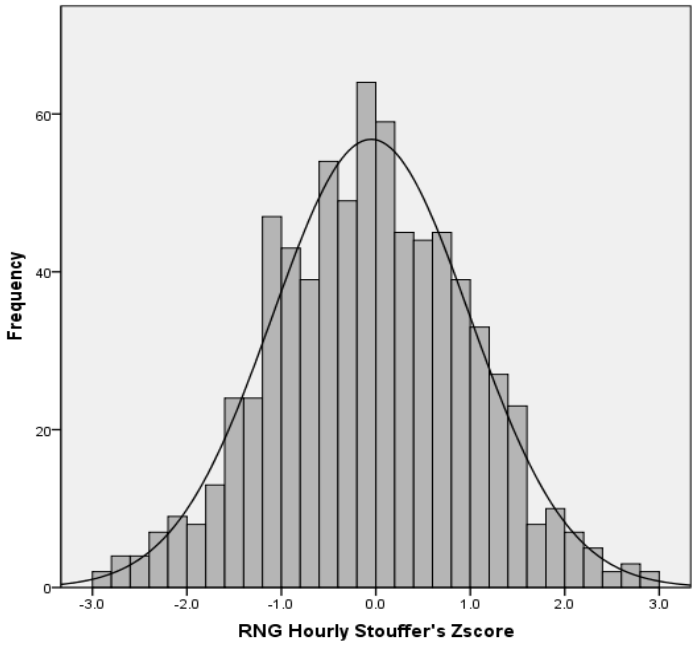


**Figure 2.3 - Display of the hourly RNG Stouffer's Cumulative Zscore frequency of occurrence for the 743 cases from January 19th, 2013 – February 19th, 2013.**

The results of the stepwise multiple regression analysis for hourly RNG z-scores and the photon power density of that hour and for each of the 72 previous hours showed that 4 variables entered the equation. These reflected the power density of photons 41, 47, 48, and 71 hours before any hourly RNG value over the 30 days. The multiple R was 0.185 and the equation [$r^2$ = .034, $F_{(4,666)}$ = 5.910, p < .001, R = .185, SEE = 1.021] accommodated ~3% of the variability in the z-scores for the hourly RNG variations. The partial slopes (partial regression coefficients) and standard errors (in parenthesis) for the four predictors were -0.075 (0.025), -0.097 (0.04), 0.136 (0.04), and 0.03 (0.016), respectively. On the other hand when the PMT data (photon flux density) was employed as the dependent variable and the RNG data for the same hour and each of the 72 hours before were entered into the multiple regression, there was *no entry* of variables. In other words photon power density primarily during the period 41 to 48 hours previously was significantly correlated with deviations in random number generation; however the hourly variation in photon measures was not significantly correlated with any of the previous hours for random number variations. Only one (lag 32) of the 72 lags for geomagnetic activity significantly predicted the RNG variations (r = -0.09).

To understand the relationship between local photon flux density and general global geomagnetic activity, their relationships were explored. When a symmetrical lag/lead equation was generated by entering the lag 24 of the hourly PMT data and 72 lags of the geomagnetic data (entry of lags <24 would indicate that future geomagnetic activity entered while lags >24 would indicate that antecedent geomagnetic activity entered) two variables entered the equation [$F_{(1,699)}$ = 16.31, p < 0.001): geomagnetic activity during the *same* hour and 10 hours previously (multiple r = 0.23). The equation (multiple r = 0.24) generated when geomagnetic data was employed as the dependent variable showed that photon flux density (partial slopes in parentheses) 10 (0.53), 28 (-0.98) and 39 (-0.73) hours previously aggregated to predict the geomagnetic (aa) values [$F_{(3,691)}$ = 14.49, p < 0.001].

By definition the correlation between the predicted values of the equation containing the four hours of previous photon data was correlated 0.19 with the hourly RNG scores. When the shared variance between the predicted geomagnetic (aa) values from photon flux density was first removed from the correlations with the actual RNG scores and predicted RNG scores, the

correlation was still significant statistically (partial r = 0.18, p < 0.001). Removing the shared variance with the actual RNG scores between the predicted RNG score and predicted aa values did not significantly change the strength of the correlations (partial r = 0.17, p < 0.001). However first removing the shared variance with the predicted RNG scores (from antecedent photon density 41, 47, 48 and 71 hours previously) reduced the partial correlation (partial r = 0.01, n. s.) between the RNG scores and the predicted aa values to a non-statistically significant level. Such results strongly suggest that recondite associations between geomagnetic activity and photon flux density were not responsible for the weak but nonetheless significant association between RNG scores and the antecedent photon fluctuations particularly about two days earlier.

The average slope for the four key hourly variables (41, 47, 48, and 71) was about 0.07. This means if valence were ignored and absolute values are only considered, every 1 unit change in photon density per minute produced a random variation changed by z = 0.08 of the total population per hour. Assuming $5 \times 10^{-11}$ W/m$^2$ and the $\sim 10^{-12}$ m$^2$ per area involved with the electron tunneling, the energy would be $5 \times 10^{-23}$ J. For a unit z shift that would be equivalent to $\sim 6.3 \times 10^{-22}$ J. This is the value predicted for the energy associated with numbers of equivalent Bohr electron energies for a deviation of more than 20 units from random number background per hour.

## 2.6 Discussion and Implications

One of the most important implications of this approach to causality of events and their influence by quantum-level energies within the two to three days before their occurrence is that single increments of energy could be the initiating sequence that could ultimately lead to the occurrence of a physical event. In other words, the collapse of a building or the failure of a biological system, such as a human being, would begin with a single, extremely small quantum of energy. If the direction of this evolving process is not disrupted within the subsequent two to three days, the event occurs in the physical time frame (the middle line in Figure 2.1). We would expect that as the statistical time approaches the manifestation of the event greater and greater amounts of energy would be required to alter or stop the occurrence of the event. Within a few moments before the event is manifested the energy requirements would approach extremely large values

and hence the event would be inevitable. This phenomenon is considered in the microscopic scale where an interaction and process can evolve. Because a physical or biological system is comprised of many evolving processes, there are many small quanta of energy that emerge, and ultimately culminate into events.

Identification or isolation of the origin of the initiating quantum of energy would significantly affect our current concepts of causality and determinism. We suggest that the origin involves the Casimir effect which is most frequently described as:

$$F_c = \hbar c \left(\frac{\pi^2}{240}\right)\left(\frac{1}{a^4}\right)(A)$$

where ħ is the modified Planck's constant, c is the velocity of light in a vacuum, "a" is the separation distance between the two plates or surfaces, and A is the area of the surfaces.

Assuming a separation between the gaps to be similar to that of the neuronal synapse (10 nm), the Casimir force ($F_c$) would be in the order 0.52 x $10^{-6}$ N and when applied over 10 nm would be 0.52 x $10^{-14}$ J. The frequency associated with this energy when multiplied by Planck's constant is 7.8 x $10^{18}$ Hz. The wave length for this frequency, assuming c, is 38 pm. This Δs is within the range of the width of a hydrogen atom and the Bohr radius.

The Casimir force has been considered to be one of the most conspicuous macroscopic manifestations of the zero point vacuum oscillations from which virtual particles become physical matter. According to Bordag et al. (2001) the geometric conditions such as the Δs associated with the electron tunneling in the RNG allow quantum electrodynamics to affect the virtual photons which constitute the field. The creation of particles from this presumed infinite vacuum energy requires the application of external fields, such as the ones employed to produce electron tunneling. Energy is transferred from this external field to the vacuum fluctuations that are the virtual particles, to transform them to actual physical entities. The boundary conditions depend upon temporal variation to produce particle creation.

The manifestation of a discrete quantum of energy ($10^{-18}$ J) equivalent to only one particle, such as the electron, has the capacity to begin the sequence of processes that ends with a physical event. At the point of this transformation from virtual to real particle there would be a substantive bifurcation of sequences. One of them reflects the results of the bifurcation in this physical world; the other would reflect what would have occurred if the transformation had not occurred. The philosophical challenge is whether or not these particles that are transformed from virtual particles have an initial determined structure that can be inferred or more optimally modified by the appropriate technology. If an electromagnetic field with a changing boundary (Bordag et al, 2001) is required to facilitate the transformation from a virtual to real particle, then circularly rotating magnetic fields with intrinsically changing angular velocity, which would accommodate the temporal-spatial requirements for this condition, could be applied to affect this "causality".

Dotta and Persinger (2009) have described a model by which an "energetic" pattern exists within the specious present during the early stages of the ~2 to 3 days that is ultimately manifested as the physical event. Dotta and Persinger correlated the global geomagnetic activity on the days of and ±3 days of events of death and crisis, or catastrophic changes in biological systems, with the global geomagnetic activity on the day of cognitive prescience of these events. Because geomagnetic activity is intercorrelated over two to three day periods, only those verified cases where the time between prescience (usually manifested as an intense dream) and the later event exceeded 5 days were explored for analyses.

Unlike the predictions one would expect if space-time were a tesseract and a geometric "twist" or back-loop occurred in this line, the maximum correlation (r~0.55) between global geomagnetic activities was not for the day of the event and the day of the experience. Instead the largest and most reliable correlation occurred between the geomagnetic activity on the day of the experience and what the geomagnetic activity would be two days *before* the event. These results, initially difficult to explain, are now quite consistent with the relationship we measured in the present experiments. The information presumably discerned a priori by a form of prescience would not have been a function of the actual event but of the energetic process or field that preceded the actual manifestation of the event.

The detection of the hypothetical energetic antecedent pattern that precedes the actual event (rather than the actual physical processes associated with the event) appears to require an altered state, such as dreaming, where photon emission and detection would be more probable. There is recent evidence that during periods when subjects are instructed to imagine white light while sitting in complete darkness, there are measurable increases in photon emissions *(*~$10^{-11}$ W/$m^2$) from the right hemisphere but not the left hemisphere. The effect is very replicable and involves energies that are within the range generated by a few million neurons, each discharging at about 10 Hz with each action potential representing ~$10^{-20}$ J (Persinger, 2010). This fundamental quantum also represents the energy associated with the distances between the potassium charges along the surface of the cell membrane that generate the resting membrane potential as well as the energies involved with the sequestering of ligands to various receptors. This value is the universal quantum unit when the estimated total force within the universe divided by the total number of Planck's voxels (unit "string" volumes) is distributed across the distance of the hydrogen line or wavelength of about 10.8 cm (Persinger et al, 2008).

The involvement of the right hemisphere as the primary source of these biophotons while imagining white light is relevant with respect to the widening of the Δt experienced as "present", because this hemisphere is preferentially activated during dreaming (Gordon et al, 1982). This was the primary state in which people reported the prescience experiences during geomagnetic conditions that was most correlated with the geomagnetic activity that preceded the actual event by about two to three days (Dotta & Persinger, 2009). This association could indicate that there is some property of photons that precede future events, which is accessible to or entangled with the photons associated with the marked visualization and imaginary processes involved with the right hemisphere during altered states such as dreaming.

A conceptually challenging implication of this approach is that the source of this "energetic" photon-related field (that can affect the cognitive, neuronal energy) that is entangled with and potentially determinant of the manifestation of the physical event may emerge from entropy within the universe. Application of the classic description of entropy of $S = ln\ g\ kT$, where k is the Boltzmann constant, T is temperature *(*~ 4ºK) and g is the degrees of freedom is the system,

is revealing. If we assume the numbers of photon equivalents in the universe is the mass of the universe ~$10^{52}$ kg (Persinger, 2009) and the upper limit of the rest mass of a photon is ~$10^{-52}$ kg there would be $10^{104}$ photons (Persinger, 2009) or degrees of freedom. The ln value is 239.47. Hence the energy associated with the threshold for entropy is about 1.3 x $10^{-20}$ J, or the energy associated with the action potentials coupled to thinking.

That thought or intention itself (which would include observation and measurement) can influence the manifestation of events or matter has been considered a viable possibility from many different perspectives. Burst spiking of a *single* cortical neuron can modify the entire global brain state (Li et al, 2009). This trigger, which would involve energies within the range of $10^{-20}$ J, switches cortical states from slow wave to rapid-eye-movement (dream) states. The quantum required is certainly within the threshold of the Landauer limit (ln 2 kT), or 2.97 x $10^{-21}$ J which is the energy involved with the loss or gain of a one bit of information or the convergence of two operations at brain temperature (*37° C*) .

Although the results of this experiment cannot fully address the energies involved with the physical process of the Δt in Figure 2.1 that constitutes the "now" of perception, there is a solution of potential relevance. Koren and Persinger (2010) applied the Casimir equation to the dimensions of the entire universe. Assuming classic total energies in the order of 1069 J and a median value for the surface area of the horizon, they calculated the estimated separation between this surface and a second concentric surface. The value was ~ 54 μm.

The estimated mass emerging per second throughout the universe would have an estimated energy equivalence between $10^{53}$ and $10^{54}$ J/s, or (assuming a volume of $10^{78}$ $m^3$ for the volume (Persinger, 2013)), about $10^{-25}$ to $10^{-26}$ J per cubic meter. When divided by Planck's constant, the resultant frequency is remarkably congruent with the GHz band of the hydrogen line. The cubic meter unit is consistent with the assumption that the general density is about 1 proton per $m^3$ (Persinger, 2009). These general quantitative values could indicate that the energy associated with the physical features of "events" is mediated universally through some discrete feature of the hydrogen atom. Considering Ernst Mach's principle of the *immanence of the universe*

whereby properties of local matter depend on the presence of the remainder of the universe, such intricate and pervasive connections between the local "now" and the whole would be consistent.

From this perspective the occurrence of the physical "now" would be our local measurement and perception of the continuous transition of virtual particles of what will happen into what is happening. The product of the gravitational constant ($6.6 \times 10^{-11}$ $m^3/kg\ s^2$) and the average density ($10^{-27}$ $kg/m^3$) of the universe results in a duration in the order of 90 billions of years (Persinger, 2012) or about 14% of the total age of the universe. The remaining time "yet to occur" represents the estimates for the proportion of dark matter and dark energy in the universe. If as suggested (Persinger, 2012) dark energy and matter represent energy and matter yet to occur, then this process of transformation would be the physical events of "now". At our $\Delta t$ and $\Delta s$ of perception (Persinger, 1999) and measurement their probability of occurring could be discernable by measuring photon densities and their temporal patterns during the previous few days.

The experimental results pertain to the atomic level and relevance for virtual-to-matter determinism. The fluctuations of photons and the outcomes of randomly generated numbers from quantum tunneling electrons were detectable by photon fluctuations at a temporal distance of 41, 47, 48, and 71 hours. The concept of causation and influential intention upon events is complimented by the theory of Topological Geometrodynamics (TGD) (Pitkänen, 1988) and the TGD Inspired Theory of Consciousness (Pitkänen, 2003). If quantum events yet to be determined are detectable from prior background photon fluctuations emerging from the background vacuum, then the causal nature of random states of energy could be reduced to be the influence of pairs of future and past directed light-cones.

If there is superposition of states decoupled from the immediate environment, regardless of space or time but with many degrees of microscopic freedom, then the macroscopic system could behave quantum mechanically. Assuming intentional actions produce energetic consequences the interpretation of the naturally occurring randomness necessarily resides within classical concepts (i.e., causation and determinism). The appropriate use of causal space-time descriptions would therefore depend upon the value and temporal direction of the quantum of action (Bohr, 1928).

**Acknowledgements**

Thanks to Professor Blake T. Dotta and Viger M. Persinger for their technical contributions.

## 2.7 Addendum

**The following comments were provided by the authors in response to a number of clarifications requested by one of the reviewers, Dr. Matti Pitkänen (MP).**

**MP**: I did not understand the theoretical considerations of the article completely and this motivated the following questions:

**Question 1.** I do not understand the motivation for the hypothesis that a phenomenon in spatial scale $\Delta x$ is discernible in time scale $\Delta t$ assuming $\Delta x/\Delta t \sim 1$ m/s. If one can bring in light velocity *c* meaning assumptions about what it is to be discernible, one has dimensionless scaling ratio $\Delta x/c\Delta t = 3.3 \times 10^7$. This would be fascinating but is there any empirical evidence for this claim?

**Response:** There is an apparent relationship between the increments of space and time pertaining to the perception of the phenomenon. If the increments are not aligned, the detection of processes which require successive temporal sequences would be summated arbitrarily and only averages could be achieved. This goes to the core argument and theme of the present investigation, which is that we are dealing with phenomena in totally different time scales, which accompany each other.

**Question 2.** The scale T = 2 days was derived as a ratio of two numbers. I did not understand the estimate: my version of the estimate gives the same number $1.6 \times 10^5$ but as a dimensionless number rather than having a unit of time (second). In more detail:

1. The first number, call it *X*, was the total energy flux for the fluctuation of background photons through a likely area of order micrometer squared of gap junction for electron tunnelling in RNG. This flux fluctuation occurred about 2 days before the RNG produced the sequence of

samples of duration of 1 second containing sequence of 200 bits. The criterion for a sample to be counted as an event was a deviation from mean of 100 1s (electron tunnelling) per second was more than 20 percent. The unit of this quantity is power (J/s). About 20 such tunnelling events per hour were observed.

2. The second number, call it *Y*, was presumably kinetic energy of electron for lowest Bohr orbit in hydrogen atom multiplied by the number 20 of events per hour(!). Also this gives a quantity with unit of power (J/s). I did not understand why this choice was made and whether it relates to electron tunnelling. In any case, the ratio *X/Y* of these two quantities with dimension of power is *dimensionless* number $X/Y = 1.6 \times 10^5$ rather than $1.6 \times 10^5$ s or 44.4 hours.

**Response:** Yes, the timescale was computed as a ratio of two numbers. The first number was derived by taking the total energy of Bohr radius electron at the fine structure velocity $4.37 \times 10^{-18}$ J. We looked at the number of occurrences of events that were of an absolute deviation from the mean by ±20 (i.e. 80 or 120) which by a mean of 100 and a standard deviation of approximately the square root of 50 is equal to a z-score of 2.86. Data was analyzed, and an average of 20.38 of these significant events occurred during a given hour, or approximately 20 of the 3600 randomly generated events. The randomly generated events are not directly representative of an individual electron, yet it was assumed that with the cascades of electrons, one would be sufficient to determine if an event was significantly deviated from the mean. So, with 20 out of a possible 3600 events being greater than an absolute deviation of z-score 2.86, multiplied by the total energy of an electron at the fine structure velocity $4.37 \times 10^{-18}$ J, yields a value of $8.74 \times 10^{-17}$ J as the total energy for significant deviations per hour.

The second number for the ratio was the photon variations per hour with the cross sectional area of the electron tunneling. Photon variations have a value of 4 to $5 \times 10^{-12}$ W/m$^2$. Multiplying this value with the assumed cross sectional area of the electron tunneling at approximately $10^{-12}$ m$^2$, yields a value of 4 to $5 \times 10^{-22}$ J/s.

The ratio between these two numbers is the representative temporal time scale of dispersion between the two devices. $8.47 \times 10^{-17}$ J divided by $4.5 \times 10^{-22}$ J/s results in $1.94 \times 10^5$ seconds or

approximately 2.25 days which is within the predictor variable hours of 2 – 3 days. Assuming a distribution of electron tunneling and significant events, the orders of magnitude remain within the 2 – 3 day period.

**Question 3.** I do not understand how the kinetic energy on Bohr orbit of atom (hydrogen?) could relate to the functioning of RNG. How could it relate to tunneling? This would require a detailed explanation.

**Response:** The phenomenon occurs with fundamental quantum units of the electron (i.e. Bohr); hence the entire universe should be considered as involved. We would have involved Mach's principle of immanence of the universe but left this perspective for another time. We had reasoned that if the product of the electron's mass ($9.1 \times 10^{-31}$ kg), fine structure velocity ($2.18 \times 10^{6}$ m/s) and neutral hydrogen line ($1.42 \times 10^{9}$ Hz, because of its immanence throughout the universe) as applied across the likely cross-sectional distance of the RNG functional tunneling width ($10^{-6}$ m) is $2.82 \times 10^{-21}$ J, it would facilitate the mechanism of an interactive representation of entropic information between the RNG and PMT devices. The energy value for a bit of information to dissipate into entropy or to appear from it according to Landauer Limit, $kT\ ln2$ or $1.38 \times 10^{-23}$ J/T multiplied by 21 degrees C (the local temperature) or 294 degrees K multiplied by 0.69 is $2.82 \times 10^{-21}$ J. In other words there is the potential (certainly not proof) for intercalation.

Relating, the time scale of sampling is 5 ms for 1 of the 200 randomly generated numbers. This sampling rate can also be manipulated with the software to collect up to 1000 numbers per second. Dr. Dotta has confirmed the analogue photomultiplier tube samples once per minute, from which the data was then used to calculate the hourly average for the statistical analysis. Verifying the duration of the photon flux fluctuation will require further investigations and has been identified as an important measure to be taken with this and future calculations.

# Chapter 3

## 3 The ~3.6 to 3.7 M Paucity in Global Earthquake Frequency: Potential Coupling to Zero Point Fluctuation Force and Quantum Energies

***International Journal of Geosciences*, 2013, 4, 1321-1325** Published Online December 2013 (http://www.scirp.org/journal/ijg) http://dx.doi.org/10.4236/ijg.2013.410127 Open Access ***IJG***

**David A. E. Vares, Michael A. Persinger**

Laurentian University, Sudbury, Canada

Email: dx_vares@laurentian.ca, mpersinger@laurentian.ca

Received October 5, 2013;

Revised November 3, 2013;

Accepted November 25, 2013



**ABSTRACT**

There has been protracted historical evidence of a relative paucity in the distribution frequency of global earthquakes within the M = 3.5 to 4.0 range. We observed a similar phenomenon for all recently recorded earthquakes from January 2009 through August 2013. Frequency distributions with increments of M = 0.1 verified the trough of the diminished incidence to be between M = 3.6 and 3.7 with an abrupt increase between M = 3.9 and 4.0. The calculated equivalent photon wavelength for the energies associated with M = 3.6 approaches Planck's Length while the related time increment is the cut-off frequency for the Zero Point Fluctuation force coupled to gravity. The conspicuous congruence between Planck's time and length and the lower than expected frequency based upon Gaussian assumptions of distribution for the discrete band of

energy associated with this magnitude range of earthquakes suggests a conduit may exist between intrinsic features of Planck space-time and geophysical processes. The existence of such a connection would encourage alternative explanations for sun-seismic activities as due to solar instabilities. Instead, it may reflect influence upon both from alterations in the structure of space being traversed by the solar system as it moves through the galaxy.

**Keywords:** Low Magnitude Earthquake Frequency; Gaussian Distribution; Planck's Length Energy; Zero Point Fluctuation Frequencies; Quantum Geophysical Effects

## 3.1 Introduction

In addition to the impacts from coronal mass ejections (Plunkett, 2000) that involve source energies in the order of $10^{25}$ Joules within a brief period, the most intense temporal increments of energy within local geophysical space are associated with seismic events. Although their lifetimes are in the order of tens of seconds, the energy release ranges from $10^{4}$ (M = 0.01) to $10^{18}$ (M = 9.0) Joules. Assuming the universal application of the central limit theorem which states that the mean of the total set of all subsets of random process should display dispersions of incidence around a central tendency that reflects a Gaussian (normal) distribution, one would predict a comparable pattern for the numbers of global earthquakes along the continuum of magnitudes. However, examination of all recorded global seismic events catalogued between January 2009 and September 2013 indicated a deviation from this prediction. In addition to a bimodal and positively skewed distribution of frequency as a function of magnitude, there was a conspicuous paucity of events from expected values that occurred within the range of 3 to 4 magnitude releases of energy.

This bimodal distribution of global seismicity was reported by Zielke and Arrowsmith (2008) for a synthetic record of 540 kyrs containing ~900,000 earthquakes with rupture areas > 5 $km^2$ or M ~ 4.5. The best fit equation for the magnitude-frequency distributions was a power law for M = 4.8 to 6.8 events with a second function to describe the event probability near M ~ 7.3. They attributed these patterns to the abrupt increase in width of the rupture at the transition between smaller and larger seismic events to the temperature dependence of the depth related changes in

friction and decrease in coseismic stress. The distinction between the two populations occurred between 11 and 12 km or about half the depth for the Curie (temperature) point for iron. With greater global coverage and sensitivity of instrumentation, unusual distributions of even smaller magnitude events have been noted. Speidel and Mattson (1983), who analyzed 10,341 earthquakes with magnitudes 2.0 to 8.2 from 1989 to 1991 revealed a conspicuous flattening of the increase in frequencies of earthquakes within a narrow interval (mean = M ~ 3.3; standard deviation = SD ~ 0.4) when the entire population between M 2 and M 8 was plotted. The other distribution anomalies were around M = 4.9 (SD = 0.5) and M = 7.1 (SD = 0.5), which was similar to the results of Zielke and Arrowsmith (2008).

There is an alternative concept to potentially explain this divergence from the normal distribution curve and implicitly, assuming random occurrences, the Central Limit Theorem. We suggest the deviations from expectation for the frequency of this increment of energy reflects focal alterations in the physical-chemical features of Earth's matter due to more fundamental and universal processes. The mass of the planet occupies space whose submatter ($<10^{-16}$ m) structure has been considered to be multidimensional with mathematical connectivity to Kaluza-Klein configurations (Reddy et. al., 2007) and physical coupling to gravity (Konstantinov, 1997) and the Zero Point (Fluctuation) Force (ZPF) of the vacuum. As aptly stated by Puthoff (1989) and Sakharov (1968) gravity is not a separately manifesting fundamental force but an induced effect associated with ZPF within the structure of space (the "vacuum"). One type of expected vacuum quantum effect is the creation of particles from the vacuum condition (Bordag et. al., 2001). If energy is transferred from an external field to vacuum oscillations, these "virtual particles" can emerge in macrospace as real increments of mass. Conversely, in a dynamic context where Newton's Third Law, for every force there is an equal and opposite force, is operative, "real" particles could be immersed into their virtual representations. A similar concept was developed by Sir Arthur Eddington (Persinger, 2013) during the early 20th century.

If the discrepancies between observed and expected frequency distributions of the release of energy by seismic events over the surface of the earth relate to quantum processes, then the wavelength of energy associated with the transition should reflect Planck's length derived from:

$$P_L = \sqrt{Ghc^{-3}}$$

where *G* is the gravitational constant, *h* is Planck's constant and *c* is the velocity of light, and, the Planck cut-off frequency of the ZPF spectrum, which is:

$$\acute{\omega}_c = \sqrt{[c^5 \cdot (\hbar G)^{-1}]}$$

where is Planck's reduced constant ($\frac{h}{2\pi}$). This is 3.442 × $10^{43}$ Hz, and, is approaching the inverse of Planck's time or, as frequency, 1.855 × $10^{43}$ Hz. Here, we present evidence of a remarkable convergence between the paucity of earthquakes within a specific band of magnitudes and the congruence of their equivalent wavelengths and quantum frequencies for both Planck's length and the discontinuity frequency of the vacuum zero-point-fluctuation.

## 3.2 Methods and Materials

All of the earthquakes recorded by USGS between 1 January 2009 and 31 August 2013 were obtained. There were a total of 483,906 events. Figure 3.1 shows the frequency of the 0.1 magnitude increments of different magnitude seismic events between 0 and 9. Because of the infrequency of events above 7, they were masked by the scaling that is dominated by less intense events. Figure 3.2 shows the amplification of the section of Figure 3.1 to reveal the sudden shift (increase) in frequencies of seismic events between 3.9 and 4 M. The trough interval was between 3.6 and 3.9 M which is congruent with the interval observed by Speidel and Mattson (1983).

## 3.3 Results

To discern a more precise range for the diminishment of the expected frequency, successive increments of 0.1 M were plotted. The results are shown in Figure 3.1. Note the bimodal distribution and the sudden increase between 3.9 and 4.0. The diminishing steps of frequency of occurrence occur between 3.6 and 3.7 M.

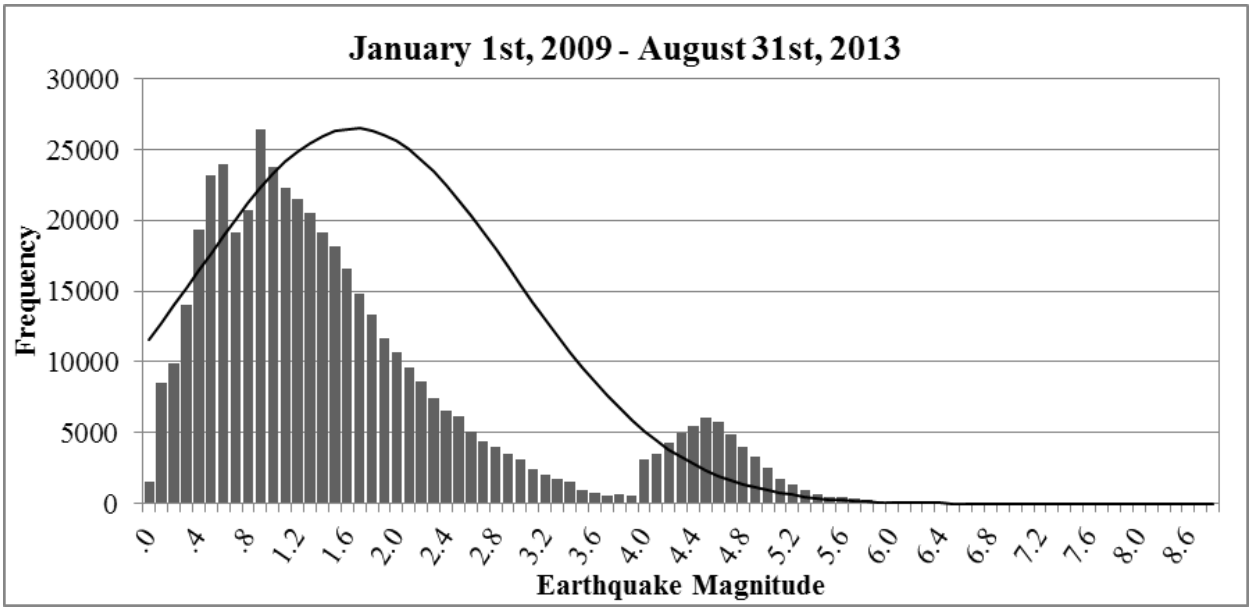


**Figure 3.1 - Total numbers of global earthquakes between January 2009 and August 2013 as a function of increments of magnitude between 0 and 9. The numbers of events above 7 are so infrequent they are masked by the scale.**

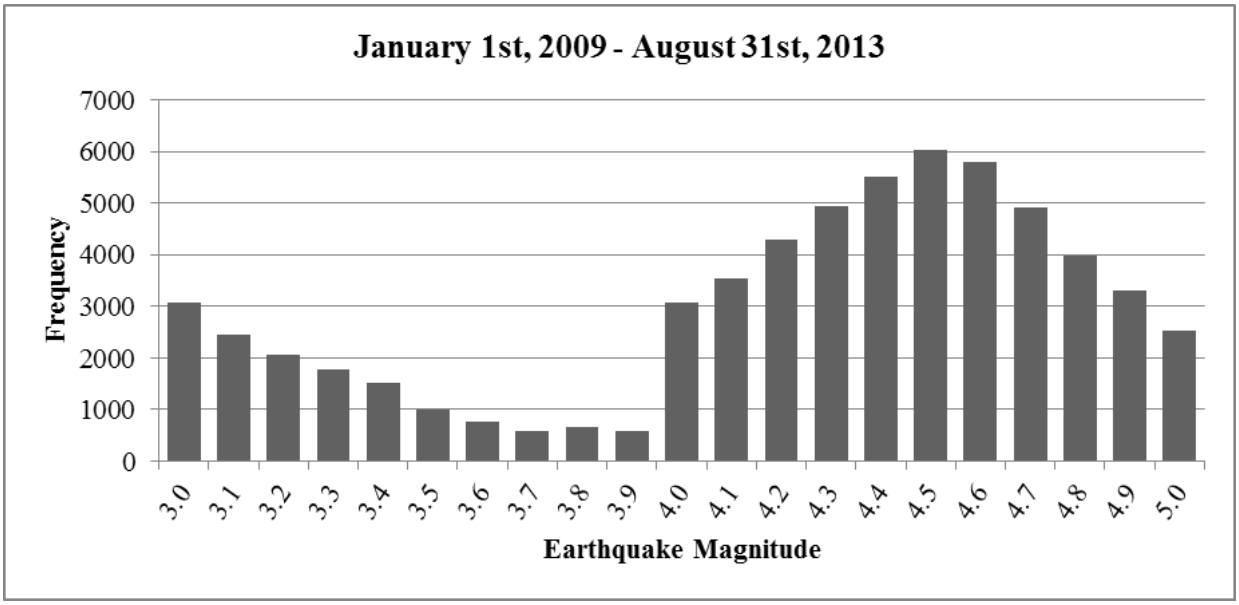


**Figure 3.2 - Amplification of the numbers of seismic events as a function of 0.1 increments of magnitude before the inflection between 3.9 and 4.**

| Earthquake Magnitude | Radiated Seismic Energy (ergs) | Radiated Seismic Energy (J) | Photon Wavelength (m) | Photon Frequency (Hz) |
|---|---|---|---|---|
| 0.01 | 6.53131E+11 | 6.5313E+04 | 3.0414E-30 | 9.8570E+37 |
| 1 | 1.99526E+13 | 1.9953E+06 | 9.9558E-32 | 3.0112E+39 |
| 2 | 6.30957E+14 | 6.3096E+07 | 3.1483E-33 | 9.5223E+40 |
| 3 | 1.99526E+16 | 1.9953E+09 | 9.9558E-35 | 3.0112E+42 |
| 3.4 | 7.94328E+16 | 7.9433E+09 | 2.5008E-35 | 1.1988E+43 |
| 3.5 | 1.12202E+17 | 1.1220E+10 | 1.7704E-35 | 1.6933E+43 |
| 3.52639 | 1.22908E+17 | 1.2291E+10 | 1.6162E-35 | 1.8549E+43 |
| 3.6 | 1.58489E+17 | 1.5849E+10 | 1.2534E-35 | 2.3919E+43 |
| 3.7 | 2.23872E+17 | 2.2387E+10 | 8.8731E-36 | 3.3787E+43 |
| 3.8 | 3.16228E+17 | 3.1623E+10 | 6.2817E-36 | 4.7725E+43 |
| 3.9 | 4.46684E+17 | 4.4668E+10 | 4.4471E-36 | 6.7413E+43 |
| 4 | 6.30957E+17 | 6.3096E+10 | 3.1483E-36 | 9.5223E+43 |
| 5 | 1.99526E+19 | 1.9953E+12 | 9.9558E-38 | 3.0112E+45 |
| 6 | 6.30957E+20 | 6.3096E+13 | 3.1483E-39 | 9.5223E+46 |
| 7 | 1.99526E+22 | 1.9953E+15 | 9.9558E-41 | 3.0112E+48 |
| 8 | 6.30957E+23 | 6.3096E+16 | 3.1483E-42 | 9.5223E+49 |
| 9 | 1.99526E+25 | 1.9953E+18 | 9.9558E-44 | 3.0112E+51 |

**Table 3.1 - Calculations for measures of energy, photon wavelength and frequency for various magnitude equivalents of earthquakes.**

In order to relate the radiated energy associated with each magnitude, we employed the Gutenberg-Richter Relation:

$$\log E = 1.5\mathrm{M} + 11.8$$

The related photon wavelength ($\lambda$) was obtained from the Planck relation of:

$$E = hc\lambda^{-1}$$

The equivalent frequency was obtained by dividing the velocity of light, c, in a vacuum (~$3.0 \times 10^8$ m/s). The results are shown in Table 1 for the range of magnitudes with particular emphasis on the magnitudes associated with the inflection threshold between 3.5 and 4.0 M. The equivalent photon $\lambda$ at ~3.6 M is remarkably similar to the $1.616 \times 10^{-35}$ m values for Planck's length.

## 3.4 Discussion and Implications

If the discrepancy in expected frequency of magnitudes of earthquakes with energetic equivalences approaches the wavelengths associated with the structure of space-time, then the source of these seismic phenomena could reflect their more cosmological connections. For example, the approximate 10 to 11 year cycle in global seismicity has been known for almost a century (Dewey, 1970). Several correlational studies have demonstrated, employing annual increments of analyses, coefficients of ~0.4 to 0.5 between the global release of seismic energy and solar activity within the 10 to 11 year cycle (Odintsov, 2007). Movement of the Sun around the barycenter of the solar system, as inferred by the absolute value in the change of the Sun's acceleration with time, was correlated 0.45 with the amount of seismic energy released from deep (>60 km) but not shallow earthquakes (Jakubcova & Pick, 1986). That planetary positions, which could potentially affect the barycenter and produce secondary electromagnetic atmospheric effects (shortwave signal quality) had been known since Nelson's classic 1952 publication (Dewey, 1970) and was recently elucidated with more rigorous mathematical and quantitative analyses by Abreu *et al.* (2012).

The temporal direction between seismic events and solar activity, although evident with analysis increments of months or years, is less clear when daily increments are employed. Sytinskij's (1989) powerful analyses of global seismicity and solar activity reiterated their large scale associations. Although the intuitive explanation was that the solar activity produced the conditions for seismic events through accelerated velocity and density of the solar wind, Sytinskij found that earthquakes *preceded* geomagnetic activity by 1 or 2 days. This relationship would be more consistent with a change within the shared Planck space-time and intrinsically gravitational associated zero point fluctuation force transiently occupied by the solar system as it moves through the galaxy.

From this perspective, the temporally discrepant elicitations of the terrestrial and solar releases of energy simply reflect their differential latencies to this third factor. There are new approaches to consider the effective coupling of gravity to matter (Balakin et. al., 2003) and sufficient

mathematical models that could test the predictions of topological transitions and large-scale space-time structure for those multidimensional theories of gravity (Reddy et. al., 2007) (Konstantinov, 1997). The existence of this connection could also accommodate some of the anomalies, namely the "stochastic fluctuations" of the dynamo driving parameters for the coupling between the minimum-maximum of the Sun's activity and the mean- field dynamo (Usoskin et. al., 2009).

There may be direct application for this explanation for the M = 3.5 window. Main (1992) reported two classes of earthquakes that preceded the explosive eruption of Mt. St. Helens on 18 May 1990. One class displayed a normal distribution of M = 4.6. The second group displayed a peak about M = 3.4, which was considered a probationary transition between being valid and an artifact of incomplete reporting. Preceding the Mt. St. Helens volcanic eruption, Derr and Persinger (1986) showed a strong temporal and spatial correlation between the occurrence of unusual luminous phenomena within the area of the Satus Peak fault zone and the inferred movement of tectonic strain associated with the later occurrence of this magnitude range of earthquakes. Interestingly, many of the historical observations of atypical pre-earthquake luminosities preceded regional smaller earthquakes with magnitudes in this range (Persinger & Derr, 2013). The involvement of Planck space-time processes could alter the interpretation of these anomalous phenomena.

Main's explanation (1992) was the bimodal peaks which were the superimposition of "tectonic" events and volcanic tremor. From the perspective of our model, if the source of the energy producing the magnitude increment is coupled to ZPF-related processes, the reversal of frequency, that is an increase in numbers of quakes, would suggest that there has been a reversal of the transformational process. Energy from the ZPF sources could then create the conditions for this magnitude band of quakes and produce this mass shift in the organization of matter. Recently, Alexeevich *et al.* (2011) have also pursued the hypothesis for the connection between seismicity of the Earth with fluctuations in the structure of physical (vacuum) space. If fundamental forces that involve gravity and the structure of space at Planck's levels are associated with the incidence rates of the narrow band of earthquake magnitudes reported here, one would expect a conspicuous connection with changes in photon emission densities

(Persinger, 2012). Interestingly, for at least two recent M > 8.0 earthquakes (Chile and Japan) several thousands of km away, we have measured marked increases in typical photon emission flux densities (~$5 \times 10^{-11}$ W/m$^2$) from the ground, by between a factor of 10 to 50 times, about two weeks before those seismic events (Persinger et. al., 2012).

# Chapter 4

## 4 Earthquakes, Human Electroencephalography, and Background Photon Fluctuations

Considering fluctuations of randomness are quantum in nature, quantum vacuum fluctuations are predictions of the quantum theory. Photo multiplier tubes (PMT) harnesses the p-n junctions and the photoelectric effect of incident background photon current measurement. Earthquake variability has been demonstrated temporal relationships with background photon fluctuations (Persinger, 2013). Similarly, human electroencephalography has also demonstrated a consistent relationship to biophoton emissions when participants engage in certain conscious activities (Dotta et. al, 2012). These seemingly random yet complex phenomena suggest an intrinsic relationship might exist between the Earth, brain activity, and light.

### 4.1 Introduction

Quantum fluctuations affect virtually all physical processes. Electric and magnetic fields of a given fluctuation frequency, obey the Heisenberg's Uncertainty Principle (1930). In the lowest state, the uncertainty in momentum and the uncertainty in position of an oscillator will still have an associated energy. Because photons can be considered to be comprised of (or at least interact with) electric and magnetic fields the random directions retains fluctuations. When considering the perspective of experience, one must introduce the concept of time to the movement. The universe is understood to be in a constant vibration of movement. Yet the temporal relationships between phenomena conform to universal properties of matter and display remarkable tendencies beyond randomness and chance expectations.

Dotta, Saroka & Persinger (2012) have reported an inverse relationship between regional cerebral voltage and right hemisphere photon emissions while participants imagined white light. With the positive relations above, external photon fluctuations are directly representative of relative left hemisphere activity while internal visualizations of photon fluctuations are inversely representative of right hemisphere activity.

Persinger, Lafreniere, and Dotta (2012) also reported significant increases in background photon emissions more than two weeks before the large magnitude Japan and Chile earthquakes. The temporal relationship suggest that amplitude changes of the recorded background photon fluctuations are potentially related to tectonic stresses of the global environment.

There exists the potential relationship between background photon fluctuations and global seismic events. Complimentary, the inverse relationship of brain activity with external photon emissions, suggest that both the local and global environment are related to background fluctuations of the electromagnetic field. There remains the cause for investigation of the 'hidden variable' that is a shared a source of variance between Earthquakes and electromagnetic brain activity.

## 4.2 Methods

### 4.2.1 Seismicity Data

The USGS Advanced National Seismic System database was queried for earthquake (EQ) data. The Advanced National Seismic System (ANSS) global composite earthquake catalogue of the U.S. Geological Survey (USGS) was accessed. For radiated energy released during an earthquake the Gutenberg-Richter Law was applied:

$$\log E = 1.5*Mw + 11.8$$

where 1.5 is the logarithmic increase, Mw is the magnitude of the earthquake, and 11.8 is a less scientific constant of a regional seismicity rate (variable by location ~ yet, this equation yields standard 6.8 Mw = 1 PJ = 1 x $10^{15}$ J). The energy calculated using this formula is measured in ergs, and is converted to Joules with the relation of 1 erg = $10^{-7}$ J.

MATLAB software was utilized to develop a programming code to calculated average and total Earthquake radiated energy as well as total numbers of recorded Earthquakes per day.

Earthquake variables were also computed for each the orders of magnitude (0.01-1 M), (1.01-2 M), etc., to above 6.01 M.

### 4.2.2 Human Electroencephalographic Data

Laurentian University's Neuroscience Research Group (NRG) maintains a database of human electroencephalographic records. The NRG Electroencephalography Database (NED) is comprised of one hundred and eighty five (185) participants for a total of two hundred and thirty eight (238) recorded sessions, occurring between June 2009 and April 2013. The procedure was approved by the university's Research Ethics Board (REB).

The majority of the participants sat in a comfortable chair in a quiet, dark room that was also a shielded acoustic chamber. An international electrode cap with 19 AgCl sensors was placed over the head and monopolar referenced to the ears. Impedance calibration was typically under 15 kOhms and maintained for each sensor. The electroencephalography (EEG) cap was connected to a Mitsar 201 amplifier system, and then connected to a portable laptop running WinEEG software used to collect the EEG data. The participants were instructed to maintained closed eyes during the duration of the record.

Artifact corrected EEG data was trimmed to 16 seconds in duration and imported into MATLAB software to calculate the spectral power densities for each of the 19 sensor channels. The data partitioned the EEG data into delta (1 - 4 Hz), theta (4 - 7 Hz), alpha 1 (7 - 10 Hz), alpha 2 (10 - 13 Hz), beta 1 (13 - 20 Hz), beta 2 (20 - 25 Hz), beta 3 (25 - 30), gamma 1 (30 - 35 Hz), and gamma 2 (35+ Hz) frequency bands.

### 4.2.3 Photon Background Data Base

The radiant power density (Watts per meter-squared) for the background photon density has been measured every minute, every day for the last four years within a basement laboratory whose floor interfaces with bedrock. The data were recorded by a RCA electron tube (photomultiplier tube, PMT) with no filters housed in a BCA IP21 unit (aperture = 12.56 $cm^2$) kept in a black

wooden box covered with 10 cm of dark cloth in a windowless dark room. The output from the PMT was transformed to millivolts for a Model 15 Photometer from SRI instruments (Pacific Photometric Instruments). The output of the PMT through the photometer was recorded and visualized once per minute by an IBM Thinkpad laptop (Windows 95). Both the photometer and computer were kept in a separate room. The sensitivity was set for 50 units for a meter that ranged from 1 to 100 units. Two methods of calibration indicated that an increase in 1 unit was approximately $5 \times 10^{-11}$ Watts per meter-squared.

## 4.3 Results

### 4.3.1 Human Electroencephalography and Background Photon Fluctuations

Correlational analyses were conducted across 9 electroencephalographic frequency band activities of the nineteen (19) sensors frequency bands power spectral density ($\mu V^2/Hz$) and the daily average photon radiant flux density revealed the following significant relations:

| Freq | Sensor | R | Rho | Sig. p < |
|---|---|---|---|---|
| (1 – 4 Hz) | Fz | -.140 | -.147 | .031 |
| (4 – 7 Hz) | Fz | -.154 | -.154 | .024 |
| (13 – 20 Hz) | Fz | -.172 | -.142 | .037 |
| (20 – 25 Hz) | Fz | -.180 | -.176 | .009 |
| (20 – 25 Hz) | F4 | -.145 | -.139 | .042 |
| (20 – 25 Hz) | Cz | -.136 | -.161 | .018 |
| (25 – 30 Hz) | Fz | -.137 | -.136 | .046 |

**Table 4.1 - Correlation coefficients between power for various frequency bands and sensor locations (Fz=frontal central; Cz is central central) from quantitative EEG measures and radiant flux density of photons.**

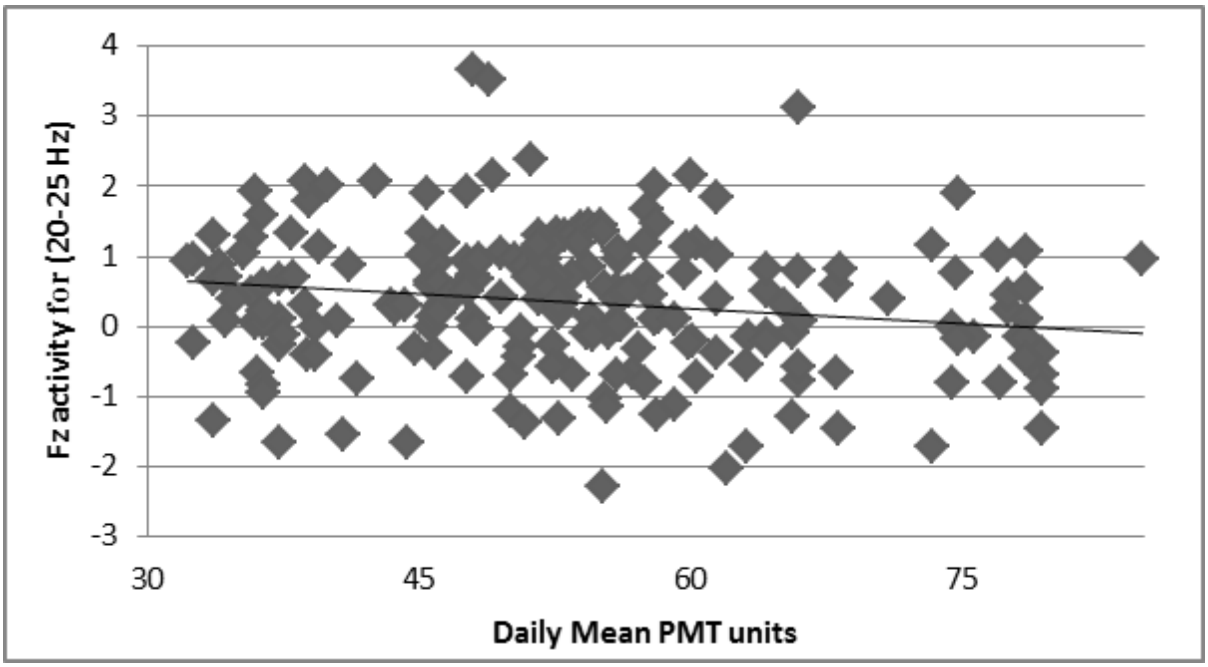


**Figure 4.1 - Relative power (Fz compared to the average microVolt measurements for all 19 sensors) of Fz within the 20-25 Hz range and photon flux density during the same period.**

The observed weak negative relationships indicate the association between the Fz sensor and the daily PMT variance (Figure 4.1 illustrates the Fz low Beta activity and PMT relation). Correlational analyses were executed for each participants (N = 216) relative sensor activity value and the daily mean PMT value (of the day of EEG recording). The following relationships were observed in Figure 4.2.

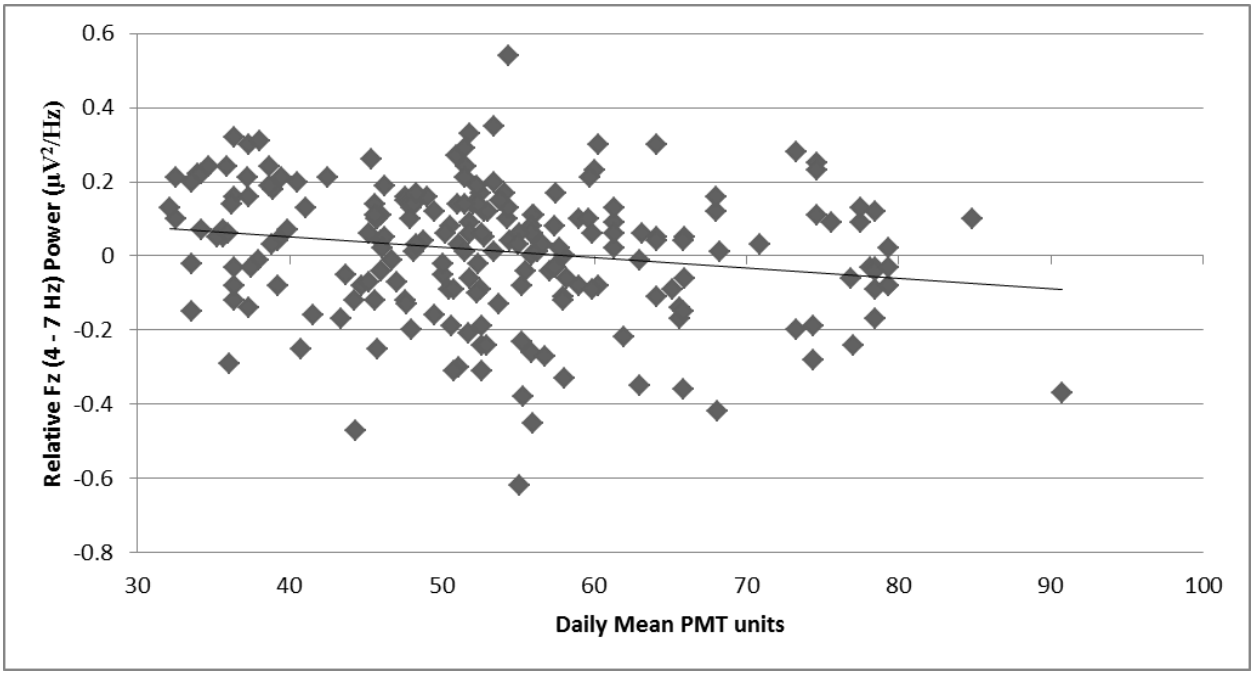


**Figure 4.2 - Relative power for frequency band 4-7 Hz (theta) within the Fz (frontal sensor) and daily photon emissions within the vicinity.**

| Freq | Sensor | R | Rho | Sig. p < |
|---|---|---|---|---|
| (1 – 4 Hz) | F3 | -.166 | -.204 | .017 |
| (1 – 4 Hz) | F4 | -.139 | -.155 | .023 |
| (1 – 4 Hz) | Cz | -.134 | -.165 | .015 |
| (1 – 4 Hz) | T5 | .173 | .166 | .014 |
| (4 – 7 Hz) | F3 | -.155 | -.152 | .025 |
| *(4 – 7 Hz) | Fz | -.199 | -.217 | .001 |
| (4 – 7 Hz) | F4 | -.178 | -.174 | .010 |
| (4 – 7 Hz) | T5 | .145 | .145 | .034 |
| (7 – 10 Hz) | Fz | -.112 | -.143 | .035 |
| (13 – 20 Hz) | Fz | -.179 | -.165 | .015 |
| (20 – 25 Hz) | Fz | -.165 | -.168 | .014 |
| (25 – 30 Hz) | Fz | -.143 | -.137 | .045 |
| (25 – 30 Hz) | Cz | -.136 | -.165 | .015 |

**Table 4.2 - Correlations between relative power in the frequency bands and photon densities.**

### 4.3.2 Human Electroencephalography and Earthquakes

Stepwise multiple regressions were conducted (3 max steps) for all $Log_{10,}$ absolute relative variables of EEG activity from the NED database with each separate order of Earthquake magnitude being held as the dependent variable. With total cases (N = 238), only days that had a total order number of Earthquakes less than +2SD were selected to account for spurious outlier cases driving relationships.

| EQ | Model F Value (sig.) | Multi R | $R^2$ | QEEG Variables | Predict R (sig.) |
|---|---|---|---|---|---|
| num0_1 | 6.94 ($1.7x10^{-4}$) | .289 | .083 | $Fp2_{(\beta)} + Fz_{(\theta)} + F3_{(\gamma)}$ | .289 ($7.5x10^{-6}$) |
| num1_2 | 7.16 ($1.3x10^{-4}$) | .295 | .087 | $P3_{(\beta)} - T5_{(\gamma)} + P3_{(\gamma)}$ | .295 ($5.5x10^{-6}$) |
| num2_3 | 11.68 ($3.8x10^{-7}$) | .366 | .134 | $- Cz_{(\theta)} - T5_{(\gamma)} + C3_{(\beta)}$ | .366 ($1.0x10^{-8}$) |
| num3_4 | 6.87 ($1.9x10^{-4}$) | .290 | .084 | $- O1_{(\alpha)} + F8_{(\theta)} - F4_{(\delta)}$ | .290 ($8.3x10^{-6}$) |
| num4_5 | | | | no variables | |
| num5_6 | 7.97 ($4.4x10^{-5}$) | .306 | .093 | $- T5_{(\delta)} + F7_{(\beta)} - P4_{(\gamma)}$ | .306 ($1.7x10^{-6}$) |

**Table 4.3 - Multiple regression analyses results demonstrating optimal combination of QEEG placements and frequencies associated with the total numbers of earthquakes in each order of magnitude.**

All predicted equations were computed and confirmed significant positive relationships between the prediction model and the daily total number of magnitude Earthquakes. The predictive scatterplots were visually inspected to ensure no outlier cases were driving the relationships.

To investigate a shared source of variance, the calculated prediction Earthquake model equations were entered into varimax rotation factor analysis. Two factors explained 50.05% of the common variance. Rotated Factor 1 loadings were represented by prediction variables for num1_2 and num2_3, while rotated Factor 2 loadings were represented by prediction variables for total number of Earthquakes of order magnitude num0_1 and num3_4.

**Rotated Component Matrix**

| | Component | |
|---|---|---|
| | 1 | 2 |
| pred0_1 | -.021 | .852 |
| pred1_2 | .796 | .237 |
| pred2_3 | .819 | -.110 |
| pred3_4 | .051 | -.566 |
| pred5_6 | .263 | -.105 |

**Table 4.4 - Rotated Factor (Varimax) factors for the five equations associating optimal combinations of QEEG measurements and the numbers of earthquakes for various integral magnitudes.**

### 4.3.3 Three-Way Partial Correlation

Controlling for outliers, cases were selected within +2 SD of the mean number of earthquakes for the different orders of magnitude. Symmetrical partial correlations were executed for the four (4) EEG predictive earthquake model equations revealing the following:

| Control Variable | Correlation Variables | R (sig.) | Partial (sig.) | Abs Δ |
|---|---|---|---|---|
| pred0_1 | pred1_2 + pred2_3 | .375 (.001) | .411 (.001) | .036 |
| | pred1_2 + pred3_4 | ns | ns | |
| | pred2_3 + pred3_4 | ns | ns | |
| pred1_2 | pred0_1 + pred2_3 | -.162 (.016) | -.242 (.001) | .080 |
| | pred0_1 + pred3_4 | ns | ns | |
| | pred2_3 + pred3_4 | ns | ns | |
| pred2_3 | pred0_1 + pred1_2 | .159 (.019) | .240 (.001) | .081 |
| | pred0_1 + pred3_4 | ns | ns | |
| | pred1_2 + pred3_4 | ns | ns | |
| pred3_4 | pred0_1 + pred1_2 | .164 (.016) | .169 (.013) | .005 |
| | pred0_1 + pred2_3 | ns | ns | |
| | pred1_2 + pred2_3 | .357 (.001) | .359 (.001) | .002 |

**Table 4.5 - Results of the partial correlation analyses between the first four equations (Table 4.3, 4.4) relating numbers of earthquakes within integer magnitudes and optimal combinations of QEEG data.**

Various associations have been previously reported including: PMT + EQ, PMT + EEG, and EEG + EQ. To investigate these associations, symmetrical partial correlations of the EEG predictive EQ num2_3 variable, EQ num2_3 variable, and the background PMT fluctuations were conducted, revealing the following:

| Control Variable | Correlation Variables | R (sig.) | Partial (sig.) | Δ |
|---|---|---|---|---|
| pred2_3 | num2_3 + PMT | .277 (.001) | .234 (.001) | -.043 |
| num2_3 | pred2_3 + PMT | .166 (.016) | .069 (.319) | -.097* |
| PMT | pred2_3 + num2_3 | .377 (.001) | .350 (.001) | -.027 |

**Table 4.6 - Results of partial correlation analyses whereby different components of the seismicity, brain activity, photon emission triad were held constant (Note: one couplet is intrinsically related by virtue of the method of regression analyses).**

## 4.4 Discussion

The brain takes in sensory information from the surrounding manifold and binds these definitions to create the functional consciousness of what has previously transpired. Somewhere throughout this process, the sensory signals to the brain are encoded with the sensory information of the body itself. We posit ourselves as a thinking being. My self-consciousness is being conscious of myself as thinking, rational being.

There is logically going to be a direct relation between the brain and the conscious mind. The brain's consciousness must have constructed itself based on what it found in the non-conscious neurological processes of connecting the chaotic sensory input. It is important to clarify here the universal link between these two concepts is not only micro and macrocosms of each other but are included in the greater macrocosm of the evolutionary dependency upon the planet Earth. Our conscious mind results from our neurological communications inside our brain and body. Our body evolved on this planet, so naturally we have similar representations within such evolution as does the planet.

The initial correlations between brain activity and background photon fluctuations would indicate that a relative decrease of the daily background photon fluctuations is representative of an increase of spectral power density activity across multiple frequency bands (delta, theta, high alpha and low beta), and would be representative of an increased experience of subjective uncertainty. The location of the Fz sensor is representative of the frontal lobe and Brodmann area 8, which is involved in frontal eye-fields and voluntary eye movements. Volz et. al. reported an increase in fMRI activation of this area when participants had to predict events with an increased experience of uncertainty. Similar relationships were observed as when not accounting for individual variability. However, two relationships were observed that had not been previous discerned involving the delta and theta relative activity over the left temporal lobe. Interestingly these were the only positive relationships observed and indicate that an increase in the daily mean PMT is related to an increase in the global-relative left temporal low frequency spectral power activity.

These results would indicate that the relative EEG predictive EQ model for Earthquakes of magnitude 2.01 – 3.00M and the daily average background photon fluctuations both share a source of variance with the total daily number of Earthquakes of magnitude 2.01 – 3.00M. Inherently, this would be due from the model of EEG activity was calculated to predict Earthquakes of that magnitude. It is the combination of a decrease of right frontal gamma, increase of right frontal beta, an increase of left frontal gamma, a decrease of right temporal gamma, and an increase of right frontal theta (for relative global activity) that is most associated the total number of daily earthquakes between the orders of magnitude (3.01 – 4M).

High frequency activity within the left hemisphere parietal, temporal, and central electroencephalographic sensor locations shared a common variance within the aggregate numbers of daily Earthquakes within orders of magnitudes between 1.01 – 3.0M. This could indicate a ‘high frequency, left hemisphere central sulcus + lateral fissure’ factor. The frontal lobes (predominantly right hemisphere), and the left occipital electroencephalographic sensor locations across multiple frequency bands loaded together as the strongest association with the total number of daily Earthquakes for orders of magnitudes between 0.01 – 1M & 3.01 – 4M and could represent a ‘variable frequency, right frontal + left occipital dipole’ factor.

# Chapter 5

# 5 Discussion

## 5.1 Central Tendency

Randomness of reality is observed throughout phenomena of the space-time manifold. Depending on the point of relative perspective, a neuronal cascade can be considered a type of random process. Yet upon changing the perspective, the seemingly electroencephalographic noise is constructed of difference patterns of frequency. The information within the stimuli and the surrounding environment is contained within the patterns of cascade. Complimented by absolute deviation from the Psyleron REG mean, earthquake, background photon emission data, additional EEG data provides effective inferential analysis to the quantum mind-matter representation phenomenon.

Random walks are fundamental to Markov processes. The outcome of a random coin toss has two possibilities, "heads" or "tails". Because the outcomes from any previous coin tosses are independent of the next, the probability of obtaining heads vs. tails will always remain 50/50 regardless of any information obtained from past toss outcomes. Thus a memoryless, stochastic process is a Markov process. Through the central limit theorem any repeated stochastic processes will lead to a Gaussian distribution. The tendency to follow the central limit theorem as N increases to infinity, the probability of a quantum random walk following the modified binary Pascal triangle increases. Photosynthesis involves quantum efficiency of a random walk. The superposition photon engages every wavefunction solution until it reaches the power source, where upon the wavefunction collapses into one, efficient path, assuring high quantum efficiency for converting light energy.

The eclectic approach employs any technique that seems best able to illuminate an aspect of a phenomenon. Likewise for inference, analysis must be conformed to scale the investigated phenomenon involved. Should sampling be variable to such an extreme degree that it cannot be ignored, then a variable length model can be employed (i.e., average number of hours of forecast rain fall, durations of atmospheric pressure).

The binomial distribution adheres to the nature of reality. Interactions of background fluctuations, quantum stochastic resonances, and even the proportions of combinations are distributed according to the central limit theorem. Fundamental stimuli and responses to these vibrational interactions eventually evolved to collapse the probability wavefunctions into one, continuous reality. Yet, the temporal relations of the interactions of randomness do not suggest a linear causation. For example at the equator, the Earth's mean rotation velocity of 1600 km/hour, the Earth's mean orbital velocity of 107,000 km/hour, the Solar System's mean motion towards Vega in the constellation Lyra of 70,000 km/hour, and the Milky Way's velocity is estimated to be 2.1 million km/hour velocity towards the constellations Leo and Virgo. A number of hidden variables may be at work in the chain of 'same temporal space'.

## 5.2 Temporal Relationships between Random Fluctuations

The REG uses two separate quantum mechanical tunneling semiconductors to initiate the instantaneous jumps of electrons across a potential barrier (also known as a band gap) between p-type and n-type heavily doped materials under a reverse-biased voltage. The randomness of electron tunneling from each shielded semiconductor undergoes a Boolean Exclusive-OR logic gate operation to eliminate environmental influence and qualify a truly randomly generated 1 or 0. The Psyleron software then treats a stream of 200 randomly generated binary bits as an event, with a natural mean of 100.

The varying voltage (white noise) generated by quantum tunneling electrons is sampled from a reverse-biased 'Field Effect Transistor' (FET). The unpredictably 'high' and 'low' voltages are due to more or less electrons tunneling across the barrier (gap junction), with a spectrum +/- 1dB, from 50 Hz to 20 kHz. A lengthy sampling procedure takes time to occur and a variability of sampled tunneling is the result. It is recommended that multiple sources of randomness (i.e., both REGs) run to cover the variable sampling issue.

The Psyleron REG device involves (2) environmentally shielded, NPN epitaxial 0.048 mg silicon transistors. Under a reversed biased current, heavily doped electrons jump across a classical barrier without loss of energy. The Heisenberg uncertainty principle grants random tunneling,

translating into a varying voltage level that is processed, amplified and converted to a digital stream. The two streams from both chips are compared with a Boolean XOR procedure to eliminate environmental influence, whereby: [(11, 10, 01, 00) = (0,1,1,0)] respectively. In short, the Psyleron REG is a professional, non-classical coin flipper.

The first study was conducted with data compiled using a quantum mechanical electron tunneling device. The jumping electron creates a varying voltage and this random process dictated a binomial distribution. Perhaps the binomial distribution is factorial, and the forces within temporal-space must not only adhere to the laws of normal distribution. They may also adhere to those forces that represent reality within human brain-space.

Yet, on a larger scale where events can appear random the center of any solar system is a quantum event generator. A proton-proton cycle produces energy within the star's core in the form of neutrinos and radiation; [$4\ {}^{1}H + 2\beta^{-} \rightarrow {}^{4}He + 2\ \nu + 6\ \gamma$]. Due to weak interactions with matter, neutrinos escape without much trouble, but as in the case of our Sun's radius, gamma radiation interacts with nearly 700,000 km of matter. Due to the conservation of energy and momentum, a photon bumping into an electron changes its path and takes time to reach the surface.

Computer simulations of the photon's quantum random walk from the center of our Sun's core traveling to the surface, is estimated to take anywhere from $(4.9 \pm 1.4) \times 10^{4}$ years for a solar constant density, and $(2.9 \pm 0.57) \times 10^{6}$ years for a linearly decreasing density. Immerging from the Sun's photosphere, an Earth bound photon takes an approximate 8 minutes to reach us. Reflection/radiation continually occurs, but the majority of photons destined for Earth undergo atmospheric refraction. The Earth absorbs $1.1 \times 10^{17}$ J/s of power from the sun. The estimated temperature of the Earth during the day is approximately 300K, while at night is around 285K. This significant range of random interaction does influence the relative perspective of the observer.

With any quantum superposition (or probability of matter collapse) exists the chance of influence from the environment system. Considering the power absorption during the Earth's day/night cycle, it is possible to suggest the effect on local randomness is influenced by the difference of

entropy entering the system. Random events on Earth and in the Sun follow universal laws and should be considered to have such relationships.

A clear gap in the numbers of earthquakes occurring within a specific range of magnitude energy is recognized. The energy representations that would otherwise be within the physical seismic activity are potentially represented within the vibrations of a photon at the Planck scale. Reports of random photon fluctuations are also related temporally to large seismic phenomena. Taken together one conclusion is that energy can be represented in different physical realities and can be represented at different temporal realities.

## 5.3 Investigating the Hidden Variable

Future analysis of quantum random fluctuations should account for or include diffusion models of neuronal cascades, correlated quantum efficiency of random walking photons, global seismicity and solar activity. Overlapping residuals of probabilities create interference patterns that collapse the wave functions. The subsequent the representation of a seemingly random and into a seemingly causal reality cannot be ignored. Perhaps the brain is a self-generating singularity capable of collapsing the quantum information obtained via the body's servomechanisms, and similarly producing external representation of reality.

Through the proportional relationships of random interaction, communication with slight manipulations of forces such as chemical, and electromagnetic fields exist. Gravity is an example. At sea level ($6.38 \times 10^6$ m from the Earth's center), a spherical diameter of 0.5 micrometers ($5 \times 10^{-7}$ m), and wet mass of about 1 picogram ($1 \times 10^{-15}$ kg) is still affected by the law of gravitation. Two simple organisms, separated at a distance of their diameter produce a gravitational force of $2.67 \times 10^{-28}$ kg m/s$^2$ (Newton). Yet, utilizing Newton's 2$^{nd}$ law, and an average Earth radius of $6.37 \times 10^6$ m, the acceleration due to the Earth's gravity at sea level to these organisms reside, the force exerted is of: $g = G(m_E/r^2)$, yielding an average value of 9.82 m/s$^2$.

When a force acts on another, the interaction fosters functional and temporal relationships. With such simple communication of entropy, these relative positions reveal patterns of our existence.

The force of gravity between the Earth and the Sun is calculated to be $3.55 \times 10^{22}$ N. The force of gravity between the Moon dominated by the Earth is calculated to be $1.99 \times 10^{26}$ N. Despite the difference in size and distance, the temporal-space required for the interaction of these forces suggest a causal sequence. The acceleration due to gravity of the Moon on objects located on the Earth's surface is approximately $3.2 \times 10^{-5}$ m/s$^2$. The changes of forces from this Moon-Earth-Sun triple conjunction during the full/new moon cycles are minuscule, but from our simple perspective, they are significant. The possible combinations and interactions within the multiverse of probabilities ripple away from conformity. Temporal-space is dilated with the masses of the above example of triple conjunction. The normal distribution of probabilities exercises kurtosis and the unlikely become probable.

Assuming linearity, the universe once a singularity, and everything (real or imaginary) has immerged from what was once contained within one central source. Without the implications of time, there was is no need for communication of information/entropy. Therefore, at the root of space-time existence resides entanglement. The residual interactions of a randomly collapsed reality merely amplify, interfere, or cohere, the already existing entanglement from which everything interacts.

So an alternative view of consciousness is that it plays the role of a buffer, only making aware to the host the bit of information that are deemed necessary and most vital to our current situation within the manifold of ongoing possibilities. Unfortunately, the illusion that consciousness is a direct comparison to the external world is very commonly accompanied with causality associations. There is a time shift in unconscious processes and what becomes aware within the conscious state. It can be substantial even at a macrocosmic level. For example Grey (2004) measured "350 milliseconds of delay between brain activity and conscious volition". The results presented above would suggest the 'hidden variable' is the relative temporal perspective of the observation.

## References


Abreu, J. A., Beer, J., Ferriz-Mas, A., McCracken, K. G., & Steinhilber, F. (2012). Is there a planetary influence on solar activity. *Astron. Astrophys*, *548*, A88.

Alexeevich, B. Y., Yur'evich, B. A., Yur'evich, Jr., B. A., Alfredovna, S. A., Arshavirovich, A. A. and Alexandrovich, S. V. (2011). Seismic Activity on the Earth, the Cosmological Vectorial Potential and Method of Short-Term Earth-quakes Forecasting. *Natural Science*. Vol. 3, No. 2, pp. 109-119.

Alpern, M., & Spencer, R. W. (1953). Variation of Critical Flicker Frequency in the Nasal Visual Field: Relation to Variation in Size of the Entrance Pupil and to Stray Light Within the Eye. *Archives of Ophthalmology*, *50*(1), 50.

Balakin, A. B., Pavón, D., Schwarz, D. J., & Zimdahl, W. (2003). Curvature force and dark energy. *New Journal of Physics*, *5*(1), 85.

Bates Jr., C. W., "Tunneling Current in Esaki Diodes," *Phys. Rev.,* 121 (1961), p. 1070.

Beck, F. (2008). Synaptic quantum tunnelling in brain activity. *NeuroQuantology*, *6*(2).

Bell, J. S. (1964). On the Einstein-Podolsky-Rosen paradox. *Physics.* ***1***, 195-200.

Berns, G. S., Cohen, J. D., & Mintun, M. A. (1997). Brain regions responsive to novelty in the absence of awareness. *Science*, *276*(5316), 1272-1275.

Bilkey, D. K. (2004). In the place space. *Science*, *305*(5688), 1245-1246.

Bohr, N. (1928). *The quantum postulate and the recent development of atomic theory* (pp. 565-88). Printed in Great Britain by R. & R. Clarke, Limited.

Bordag, M., Mohideen, U., & Mostepanenko, V. M. (2001). New developments in the Casimir effect. *Physics reports*, *353*(1), 1-205.

Burke, R. C., & Persinger, M. A. (2013). Convergent Quantitative Solutions Indicating the Human Hippocampus as a Singularity and Access to Cosmological Consciousness. *NeuroQuantology*, *11*(1).

Buzsáki, G. (2002). Theta oscillations in the hippocampus. *Neuron*, *33*(3), 325-340.

Dailey, M. E., & Smith, S. J. (1996). The dynamics of dendritic structure in developing hippocampal slices. *The Journal of neuroscience*, *16*(9), 2983-2994.

Derr, J. S., & Persinger, M. A. (1986). Luminous phenomena and earthquakes in southern Washington. *Experientia*, *42*(9), 991-999.

Dewey, E. R. (1970). *Cycles: Selected Writings*. Foundation for the Study of Cycles.

Dotta, B.T., Buckner, C., Lafrenie, R., Persinger, M. A., (2011). Photon emissions from human brain and cell culture exposed to distally rotating magnetic fields shared by separate light-stimulating brains and cells. Brain Res. 1388, pg. 77-88.

Dotta, B. T.; Persinger, M. A. (2009). Dreams, time distortion and the experience of future events: a relativistic, neuroquantal perspective. *Sleep Hypn.* ***11***, 29-38.

Dotta, B. T., Saroka, K. S., & Persinger, M. A. (2012). Increased photon emission from the head while imagining light in the dark is correlated with changes in electroencephalographic power: Support for Bókkon's Biophoton Hypothesis. *Neuroscience letters*, *513*(2), 151-154.

Di Biase, F. (2009). Quantum-holographic informational consciousness. *NeuroQuantology*, *7*(4). Engert, Florian, and Tobias Bonhoeffer. "Dendritic spine changes associated with hippocampal long-term synaptic plasticity." *Nature* 399.6731 (1999): 66-70.

Eskai, L., "New Phenomenon in Narrow Germanium P-N Junction," *Phys. Rev.*,109 (1958), p. 603.

Esaki, L. (1976). Discovery of the tunnel diode. *IEEE Trans.* ***23***, 644-647.

Ficek, Zbigniew., "Quantum Entanglement and Disentanglement of Multi-Atom System," *Quant. Phys.*, (2010).

Gordon, H. W.; Frooman, B.; Lavie, P. (1982). Shift in cognitive asymmetries between waking from REM and NREM sleep. *Neuropsychol.* ***20***, 99-103.

Grady, C. L., McIntosh, A. R., Horwitz, B., Maisog, J. M., Ungerleider, L. G., Mentis, M. J., & Haxby, J. V. (1995). Age-related reductions in human recognition memory due to impaired encoding. *Science*, *269*(5221), 218-221.

Gray, Jeffray. (2004). *Consciousness: creeping up on the hard problem.* New York: Oxford University Press

Greenough, W. T.. (1984). Structural correlates of information storage in the mammalian brain: a review and hypothesis. Trends in Neuroscience. 7.7: 229-233.

Heisenberg, W. (1930). *The physical principles of the quantum theory* (No. EPFL BOOK-106131). Dover.

Izquierdo, I., & Medina, J. H. (1997). Memory formation: the sequence of biochemical events in the hippocampus and its connection to activity in other brain structures. *Neurobiology of learning and memory*, *68*(3), 285-316.

Jakubcová, I., Pick, M., & Kárník, R. V. (1986). Is there any relation between the sun's motion

and global seismic activity?. *Studia Geophysica et Geodaetica*, *30*(2), 148-152.

John, E. R., Tang, Y., Brill, A. B., Young, R., & Ono, K. (1989). Double-labeled metabolic maps of memory. *Neurobiology of Learning and Memory*, *2*, 397.

Kane, E. O., "Theory of Tunneling", *Appl. Phys.*,32 (1961).

Kardar, Mehran., "The 'Friction' of Vacuum, and Other Fluctuation-Induced Forces," *Rev. Mod. Phys.*,71 (1999), p. 1233-1245.

Koch, C., Zador, A., & Brown, T. H. (1992). Dendritic spines: convergence of theory and experiment. *Science*, *256*(5059), 973-974.

Koenig, T., Prichep, L., Lehmann, D., Sosa, P. V., Braeker, E., Kleinlogel, H., ... & John, E. R. (2002). Millisecond by millisecond, year by year: normative EEG microstates and developmental stages. *Neuroimage*, *16*(1), 41-48.

Konstantinov, M. Y. (1997). Topological transitions and large-scale structure of space-time in multi-dimensional theory of gravity. *Russian Physics Journal*,*40*(2), 124-128.

Koren, S. A.; Persinger, M A. (2010). The Casimir force along the universal boundary: quantitative solutions and implications. *J. Phys. Astrophys. Phys. Cosmol.* ***4***, 1-4.

Korotaev, S. M.; Morozov, A. N.; Serdyuk, V. O.; Gorohov, J. V.; Machinin, V. A. (2005). Experimental study of macroscopic nonlocality of large-scale natural dissipative processes. *NeuroQuantology.* ***4***, 275-94.

Lambson, B., Carlton, D., Bokor, J.. (2011) Exploring the Thermodynamic Limits of Computation in Integrated Systems: Magnetic Memory, Nanomagnetic Logic, and the Landauer Limit. *Physical Review Letters.* 107.

Landauer, R. (1989). Barrier traversal time. *Nature.* ***341***, 567-568.

Lavallee, C. F., & Persinger, M. A. (2010). A LORETA study of mental time travel: Similar and distinct electrophysiological correlates of re-experiencing past events and pre-experiencing future events. *Consciousness and cognition*,*19*(4), 1037-1044.

Lehmann, D., Strik, W. K., Henggeler, B., Koenig, T., & Koukkou, M. (1998). Brain electric microstates and momentary conscious mind states as building blocks of spontaneous thinking: I. Visual imagery and abstract thoughts. *International Journal of Psychophysiology*, *29*(1), 1-11.

Li, C.T.; Poo, M.; Dan Y. (2009). Burst spiking of a single cortical neuron modifies global brain state. *Science*, ***324***, 643-645.

Llinas, R. R., & Ribary, U. (1992). Rostrocaudal scan in human brain: a global characteristic of the 40-Hz response during sensory input. *Induced rhythms in the brain*, 147-154.

Mach, Q. H., &Persinger, M. A. (2009). Behavioral changes with brief exposures to weak magnetic fields patterned to stimulate long-term potentiation. *Brain research*, *1261*, 45-53.

Main, I. G. (1987). A characteristic earthquake model of the seismicity preceding the eruption of Mount St. Helens on 18 May 1980. *Physics of the earth and planetary interiors*, *49*(3), 283-293.

Maletic-Savatic, M., Malinow, R., & Svoboda, K. (1999). Rapid dendritic morphogenesis in CA1 hippocampal dendrites induced by synaptic activity. *Science*, *283*(5409), 1923-1927.

Martin, T.; Landauer, R. (1992). Time delay of evanescent electromagnetic waves and the analogy of particle tunneling. *Physic. Rev.* ***45***, 2611.

Middleton, J. W., Omar, C., Doiron, B., & Simons, D. J. (2012). Neural correlation is stimulus modulated by feedforward inhibitory circuitry. *The Journal of Neuroscience*, *32*(2), 506-518.

Minakov, A. A.; Nikolaenko, A. P.; Rabinovich, L. M. (1992). Gravitational-to-electromagnetic wave conversion in electrostatic field of earth-ionosphere resonator. *Radiofiz.* ***35***, 915-923.

Moddel, G., Zhu, Z., Curry, A. M.. 2011. *Laboratory Demonstration of Retroactive Influence in a Digital System*. AIP Conf. Proc..1408, pp. 218-231.

Moser, M. B., Trommald, M., & Andersen, P. (1994). An increase in dendritic spine density on hippocampal CA1 pyramidal cells following spatial learning in adult rats suggests the formation of new synapses. *Proceedings of the National Academy of Sciences*, *91*(26), 12673-12675.

Nikonenko, I., Jourdain, P., Alberi, S., Toni, N., & Muller, D. (2002). Activity-induced changes of spine morphology. *Hippocampus*, *12*(5), 585-591.

Nimchinsky, E. A., Sabatini, B. L., & Svoboda, K. (2002). Structure and function of dendritic spines. *Annual review of physiology*, *64*(1), 313-353.

Nunez, P. L. (1995). *Neocortical dynamics and human EEG rhythms*. Oxford University Press, USA.

Odintsov, S. D., Ivanov-Kholodnyi, G. S., & Georgieva, K. (2007). Solar activity and global seismicity of the earth. *Bulletin of the Russian Academy of Sciences: Physics*, *71*(4), 593-595.

Persinger, M. A. (1999). Is there more than one source for the temporal binding factor for human consciousness?. *Perceptual and Motor Skills*, *89*(3f), 1259-1262.

Persinger, M. A. (1999). On the nature of space-time in the perception of phenomena in Science. *Percep. Mot. Skil.* ***88,*** 1210-1216.

Persinger, M. A., & Koren, S. A. (2007). A theory of neurophysics and quantum neuroscience: implications for brain function and the limits of consciousness. *International Journal of Neuroscience*, *117*(2), 157-175.

Persinger, M. A.; Koren, S. A.; Lafreniere, G. F. (2008). A neuroquantological approach to how human thought might affect the universe. *Neuroquantol. 6*, 369-378.

Persinger, M. A. (2009). A simple estimate for the mass of the universe: dimensionless Parameter A and the construct of "pressure". *J. Phys. Astrophys. Phys. Cosmol.* ***3***, 1-3.

Persinger, M. A. (2010). $10^{-20}$ Joules as a neuromolecular quantum in medicinal chemistry: an alternative approach to myriad molecular pathways. *Cur. Med. Chem.* ***45***, 940-948.

Persinger, M. A., & Lavallee, C. F. (2010). Theoretical and experimental evidence of macroscopic entanglement between human brain activity and photon emissions: implications for quantum consciousness and future applications. *Journal of Consciousness Exploration & Research*, *1*(7).

Persinger, M. A. (2011). Electromagnetic bases of the universality of the characteristics of consciousness: quantitative support. *J. Cosmol*, *14*.

Persinger, M. A. (2012). Annual variation of local photon emission's spectral power within the mHz range overlaps with seismic-atmospheric acoustic oscillations. *Int. J. Geosci.* ***3***, 192-194.

Persinger, M. A. (2012). Brain activity and lightning: potentially congruent scale-invariant quantitative properties. *Front. Integ. Neurosci*.

Persinger, M. A. (2012). Convergent calculations that dark solutions are reflective of mass-energy yet to occur. *Int. J. Astron. Astrophys.* ***2***, 125-128.

Persinger, M. A. (2012). Potential origins of a quantitative equivalence between gravity and light. *Open Aston. J.* ***5***, 41-43.

Persinger, M. A.; Lafreniere, G. F.; Dotta, B. T. (2012). Marked increases in background photon emissions in Sudbury, Ontario more than two weeks before the magnitude >8.0 earthquakes in Japan and Chile. *Int. J. Geosci.* ***3***, 627-629.

Persinger, M. (2012). The (Sum of n) = n Concept And the Quantitative Support for the Cerebral-Holographic and Electromagnetic Configuration of Consciousness. *Journal of Consciousness Studies*, *19*(11-12), 11-12.

Persinger, M. A. (2012). Potential origins of a quantitative equivalence between gravity and light. *The Open Astron J*, *5*, 41-43.

Persinger, M. A. (2013). Support for Eddington's Number and his approach to astronomy: recent developments in the physics and chemistry of the human brain. *Int. Let. Chem. Phys. Astron.* ***8***, 8-19.

Persinger, M. A., & Derr, J. S. (2013). Luminous Shapes with Unusual Motions as Potential Predictors of Earthquakes: A Historical Summary of the Validity and Application of the Tectonic Strain Theory. *International Journal of Geosciences*, *4*, 387.

Petsche, H., Stumpf, C., & Gogolak, G. (1962). The significance of the rabbit's septum as a relay station between the midbrain and the hippocampus I. The control of hippocampus arousal activity by the septum cells. *Electroencephalography and clinical neurophysiology*, *14*(2), 202-211.

Pitkänen, M. (1988). Topological Geometrodynamics. *Annalen der Physik*,*500*(3), 235-248.

Pitkänen, M. (2003). TGD Inspired Theory of Consciousness. *NeuroQuantology*,*1*(1), 68-93.

Plunkett, S. P., & Wu, S. T. (2000). Coronal mass ejections (CMEs) and their geoeffectiveness. *Plasma Science, IEEE Transactions on*, *28*(6), 1807-1817.

Puthoff, H. E. (1989). Gravity as a zero-point-fluctuation force. *Physical review A*, *39*(5), 2333.

Rall, W., & Segev, I.. "Dendritic spine synapses, excitable spine clusters and plasticity." *Cellular Mechanisms of Conditioning and Behavioral Plasticity, Plenum Publishing Corp, New York* (1988): 221-236.

Reddy, D. R. K., Naidu, R. L., Rao, S. A., & Devi, K. N. (2007). A higher-dimensional string cosmological model in Brans–Dicke theory of gravitation. *Astrophysics and Space Science*, *310*(3-4), 177-180.

Rowlands, P. (1992). The cosmological implications of nonlocal gravity. *Hadronic J.* ***35***, 557-591.

Sakharov, A. D. (1968). ZPF Theory. *Soviet Physics*, Vol. 12, pp. 1040-1045.

Sejnowski, T. J., &Destexhe, A. (2000). Why do we sleep?. *Brain research*,*886*(1), 208-223.

Speidel, D. H., & Mattson, P. H. (1993). The polymodal frequency-magnitude relationship of earthquakes. *Bulletin of the Seismological Society of America*,*83*(6), 1893-1901.

Stahlhofen, A. A.; Nimtz, G. (2006*).* Evanescent modes are virtual photons, *Europhys. Let.* ***76***, 189–195.

Symul, T., Assad, S. M., Lam, P. K.. (2011). Real time demonstration of high bitrate quantum random number generation with coherent laser light. *Applied Physics Letters*.98, 231103.

Sytinskij, A. D. (1989). Correlation of earthquakes with solar activity. *Izvestiya Physics of the Solid Earth*, *25*, 86-98.

Thomas E. Hartman 1962 Tunneling of a Wave Packet J. Appl. Phys. 33, 3427

Tononi, G., & Edelman, G. M. (1998). Consciousness and complexity. *Science*, *282*(5395), 1846-

1851.

Tsang, E. W., Koren, S. A., & Persinger, M. A. (2004). Power increases within the gamma range over the frontal and occipital regions during acute exposures to cerebrally counterclockwise rotating magnetic fields with specific derivatives of change. *International Journal of Neuroscience*, *114*(9), 1183-1193.

Tu, L. C.; Luo, J.; Gilles, G. T. (2005). The mass of the photon. *Rep. Prog. Phys.* ***68***, 77-130.

Ungerleider, L. G. (1995). Functional brain imaging studies of cortical mechanisms for memory. *Science*, *270*(5237), 769-775.

Usoskin, I. G., Sokoloff, D., & Moss, D. (2009). Grand Minima of solar activity and the mean-field dynamo. *Solar Physics*, *254*(2), 345-355.

Vares, D. A. E., & Persinger, M. A. (2013). The~ 3.6 to 3.7 M Paucity in Global Earthquake Frequency: Potential Coupling to Zero Point Fluctuation Force and Quantum Energies. *International Journal of Geosciences*, *2013*.

Vladmirskii, B. M. (1995). Measurements of gravitational constant and heliogeophysical electromagnetic perturbations. *Biophys.* ***40***, 915-213.Ross, C. T., & Redpath, S. F. (2009). Physical Formation of Memory: The Role of Glia Cells. *NeuroQuantology*, *7*(4).

Volz, K. G., Schubotz, R. I., & Cramon, D. (2005). Variants of uncertainty in decision making and their neural correlates. *Brain research bulletin*, *67*(5), 403-412.

Vos, M. H., Rappaport, F., Lambry, J. C., Breton, J., & Martin, J. L. (1993). Visualization of coherent nuclear motion in a membrane protein by femtosecond spectroscopy. *Nature*, *363*, 320-325.

Wackermann, J. (1999). Towards a quantitative characterization of functional states of the brain: from the non-linear methodology to the global linear description. *International Journal of Psychophysiology*, *34*(1), 65-80.

Wheeler, M. A., Stuss, D. T., & Tulving, E. (1997). Toward a theory of episodic memory: the frontal lobes and autonoetic consciousness. *Psychological bulletin*, *121*(3), 331.

Whitlock, J. R., Heynen, A. J., Shuler, M. G., & Bear, M. F. (2006). Learning induces long-term potentiation in the hippocampus. *Science Signalling*,*313*(5790), 1093.

Zielke, O., & Arrowsmith, J. R. (2008). Depth variation of coseismic stress drop explains bimodal earthquake magnitude-frequency distribution. *Geophysical Research Letters*, *35*(24).